Journal of Computational and Applied Mathematics 377 (2020) 112865

Contents lists available at ScienceDirect

Journal of Computational and Applied Mathematics

journal homepage: www.elsevier.com/locate/cam

Numerical computation of the capacity of generalized condensers

Mohamed M.S. Nasser [a,*], Matti Vuorinen [b]

[a] Department of Mathematics, Statistics and Physics, Qatar University, P.O. Box 2713, Doha, Qatar
[b] Department of Mathematics and Statistics, University of Turku, Turku, Finland

ARTICLE INFO

Article history:
Received 8 August 2019
Received in revised form 29 February 2020

MSC:
65R20
65E05
30C85
31A15

Keywords:
Conformal capacity
Boundary integral equations
Numerical conformal mapping

ABSTRACT

We present a boundary integral method for numerical computation of the capacity of generalized condensers. The presented method applies to a wide variety of generalized condenser geometry including the cases when the plates of the generalized condenser are bordered by piecewise smooth Jordan curves or are rectilinear slits. The presented method is used also to compute the harmonic measure in multiply connected domains.

1. Introduction

The conformal capacity of condensers is an important notion in geometric function theory [1–7] and in various applications of electronics. However, the analytic forms of the capacity are known only for special types of condensers. So, the use of numerical methods for computing the capacity is unavoidable in many applications. Indeed, numerical computation of the capacity of condensers has been intensively studied in the literature, see e.g., [3,8–11]. The capacity of condensers is one of the several "conformal invariants" which are powerful tools in complex analysis. Some of the other important examples of conformal invariants are the harmonic measure, the logarithmic capacity, the extremal length, the reduced extremal length, and the hyperbolic distance [1,4,7,12–14]. Numerical computing of such invariants has been studied also in the literature, see e.g., [6,8,15–17].

The capacity of generalized condensers is another important example of conformal invariants [4,7,18–20]. In this paper, we present a numerical method for computing the capacity of generalized condensers. We consider the case in which the plates of the generalized condensers are bordered by piecewise smooth Jordan curves or are rectilinear slits. As far as we know, the proposed method is the first numerical method for computing the numerical values of the capacity of the generalized condensers. The boundary integral equation with the generalized Neumann kernel [21,22] plays a key role in developing our method. The presented method can be used also to compute the harmonic measure in multiply connected domains.

Let B be an open subset of $\overline{\mathbb{C}} = \mathbb{C} \cup \{\infty\}$. If $B \neq \mathbb{C}$, we assume that B is either a bounded or an unbounded multiply connected domain of connectivity $\ell \geq 1$ bordered by ℓ piecewise smooth Jordan curves with $\infty \in B$ whenever B is

* Corresponding author.
E-mail addresses: mms.nasser@qu.edu.qa (M.M.S. Nasser), vuorinen@utu.fi (M. Vuorinen).

https://doi.org/10.1016/j.cam.2020.112865
0377-0427/

unbounded. If $B = \mathbb{C}$, we define $\ell = 0$. We consider generalized condensers of the form $C = (B, E, \delta)$ where $E = \{E_k\}_{k=1}^m$, $m \geq 2$, is a collection of nonempty closed pairwise disjoint sets $E_k \subset B$ and $\delta = \{\delta_k\}_{k=1}^m$ is a collection of real numbers containing at least two different numbers. The set $G = B \backslash \cup_{k=1}^m E_k$ is called the field of the condenser C, the sets E_k are the plates of the condenser, and the numbers δ_k are the levels of the potential of the plates E_k, $k = 1, 2, \ldots, m$ [4, p. 12]. We assume that G is a finitely connected domain without isolated boundary points and that $\partial G \cap \left(\cup_{k=1}^m E_k\right)$ consists of m piecewise smooth Jordan curves. Then the conformal capacity of C, cap(C), is given by the Dirichlet integral [4, p. 13, p. 305]

$$\text{cap}(C) = \iint_G |\nabla u|^2 dxdy \tag{1}$$

where u is the potential function of the condenser C, i.e., u is continuous in $\overline{G}$, harmonic in G, and equal to δ_k on ∂E_k for $k = 1, 2, \ldots, m$ and satisfies $\partial u/\partial \mathbf{n} = 0$ on $\partial B \backslash \cup_{k=1}^m E_k$ where $\partial u/\partial \mathbf{n}$ denotes the directional derivative of u along the outward normal. If G is unbounded, we assume u is bounded at ∞.

The analytical description of the problem is given in Section 2 and it is based on the classical theory of integral equations [23] and on the definition of the generalized capacity due to V. Dubinin [4]. In Section 3 we formulate the computational problem as a Riemann–Hilbert problem and prove a preliminary analytical result. A boundary integral method for solving the formulated Riemann–Hilbert problem is presented in Section 4. The method is based on the boundary integral equation with the generalized Neumann kernel [21,22]. The main theoretical results are presented in Section 5 and they deal with the unique solvability of algebraic linear systems related to the Riemann–Hilbert problem. Also an outline of an algorithm for the numerical solution of the integral equation is given. In Section 6 we give a numerical implementation of the algorithm. The code of a MATLAB implementation of the algorithm is given in Appendix. This algorithm is tested in Section 7 in the case of capacity computation of condensers with piecewise smooth boundary curves and results are compared, with good agreement of results, to earlier numerical results from [9]. In Section 8 we apply the algorithm for the computation of the capacity of generalized condensers. In Section 9, we use the presented algorithm with the help of conformal mappings to compute the capacity of rectilinear slit condensers. In the final Section 10 we show that the same method also works for the computation of the harmonic measure.

2. The potential function

We assume that $E_k = \overline{G_k}$ where G_k is a simply connected domain bordered by a piecewise smooth Jordan curve Γ_k for $k = 1, 2, \ldots, m$ (condensers whose plates E_k are slits will be handled later with the help of conformal mappings). If $B \neq \mathbb{C}$, we assume that the ℓ boundary components of B are piecewise smooth Jordan curves Γ_k for $k = m+1, m+2, \ldots, m+\ell$. Then, the field of the condenser is the multiply connected domain G of connectivity $m + \ell$ bordered by

$$\Gamma = \partial G = \bigcup_{k=1}^{m+\ell} \Gamma_k,$$

where the orientation of the curves Γ_k is such that G is always on the left of Γ_k for $k = 1, 2, \ldots, m + \ell$. For each $k = m+1, m+2, \ldots, m+\ell$, the simply connected domain on the right of Γ_k will be denoted by G_k. Thus, based on the boundedness of the domains B and G, we have the following three cases:

1. The domain G is unbounded:
   For this case, the domain B is also unbounded, since $G \subset B$, and all the simply connected domains $G_1, G_2, \ldots, G_{m+\ell}$ are bounded. Here, we assume that $\infty \in G$. See Fig. 1.
2. The domain B is bounded:
   We assume that the external boundary component of B is $\Gamma_{m+\ell}$. Hence, the simply connected domain $G_{m+\ell}$ on the right of $\Gamma_{m+\ell}$ is unbounded with $\infty \in G_{m+\ell}$. For this case, the domain G is also bounded since $G \subset B$. Further, $\Gamma_{m+\ell}$ is the external boundary component of G and encloses all the other curves $\Gamma_1, \ldots, \Gamma_{m+\ell-1}$. See Fig. 2.
3. The domain B is unbounded and the domain G is bounded:
   Since B is unbounded and G is bounded, then one of the curves $\Gamma_1, \ldots, \Gamma_m$ must be the external boundary component of G. We assume it is Γ_m. Hence the curve Γ_m enclose all the other curves $\Gamma_1, \ldots, \Gamma_{m-1}, \Gamma_{m+1}, \ldots, \Gamma_{m+\ell}$ and the simply connected domain G_m on the right of Γ_m is unbounded with $\infty \in G_m$. See Fig. 3.

For the above three cases, we define the integers m' and l' by

$$m' = \begin{cases} m-1, & \text{if } G \text{ is bounded and } B \text{ is unbounded,} \\ m, & \text{otherwise,} \end{cases} \tag{2}$$

and

$$\ell' = \begin{cases} \ell-1, & \text{if } G \text{ is bounded and } B \text{ is bounded,} \\ \ell, & \text{otherwise.} \end{cases} \tag{3}$$

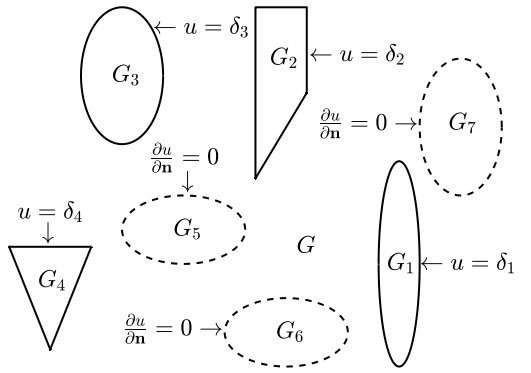

Fig. 1. An example of an unbounded multiply connected domain G for $m = 4$ and $\ell = 3$ for Case I (both G and B are unbounded).

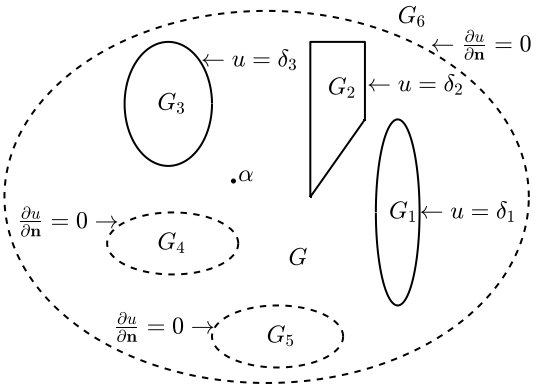

Fig. 2. An example of a bounded multiply connected domain G for $m = 3$ and $\ell = 3$ for Case I (both G and B are bounded).

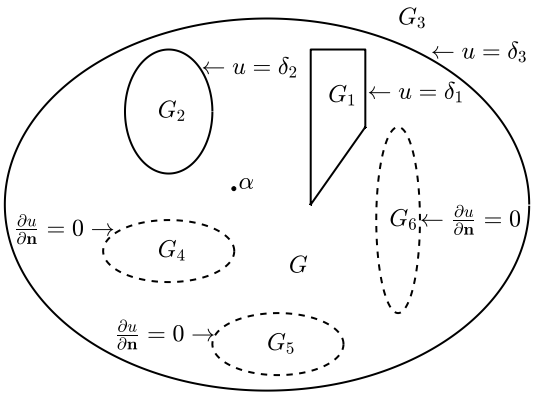

Fig. 3. An example of a bounded field of the condenser G for $m = 3$ and $\ell = 3$ for case II ($m' = m - 1$, $\ell' = \ell$).

In particular, if G is unbounded, then B is unbounded, $m' = m$, $\ell' = \ell$, and hence $m' + \ell' = m + \ell$. If G is bounded, then either $m' = m - 1$ or $\ell' = \ell - 1$ and hence $m' + \ell' = m + \ell - 1$. Further, $m' = m - 1$ means that Γ_m is the external boundary component of G. Similarly, $\ell' = \ell - 1$ means that the external boundary component of G is $\Gamma_{m+\ell}$. With these definitions of m' and ℓ', the domains $G_1, \ldots, G_{m'}$ and $G_{m+1}, \ldots, G_{m+\ell'}$ are bounded simply connected domains.

The potential function u is then a solution of the Laplace equation $\Delta u = 0$ with the mixed Dirichlet–Neumann boundary condition

$$u(\zeta) = \delta_k, \quad \zeta \in \Gamma_k, \quad k = 1, 2, \ldots, m, \tag{4a}$$

$$\frac{\partial u}{\partial \mathbf{n}}(\zeta) = 0, \quad \zeta \in \Gamma_k, \quad k = m+1, m+2, \ldots, m+\ell. \tag{4b}$$

Note that the boundary value problem (4) reduces to a Dirichlet problem for $\ell = 0$. Note also that the problem (4) does not reduce to a Neumann problem since $m \geq 2$. The problem (4) has a unique solution u [24].

A more general form of such a mixed boundary value problem has been considered in [24] using a Cauchy integral method and in [25,26] using the boundary integral equation with the generalized Neumann kernel. Due to the simple forms of the boundary conditions in (4), the method presented in [25,26] will be further simplified in this paper to obtain a simple, fast, and accurate method for computing the potential function u and the capacity $\mathrm{cap}(C)$ of the generalized condenser C.

The harmonic function u is the real part of an analytic function F in G which is not necessarily single-valued. Assume that α_k is an auxiliary point in G_k for each $k = 1, 2, \ldots, m'$ and β_k is an auxiliary point in G_{m+k} for each $k = 1, 2, \ldots, \ell'$. Then the function F can be written as [13,23,27,28]

$$F(z) = g(z) - \sum_{k=1}^{m'} a_k \log(z - \alpha_k) - \sum_{k=1}^{\ell'} b_k \log(z - \beta_k) \tag{5}$$

where g is a single-valued analytic function in G and $a_1, \ldots, a_{m'}, b_1, \ldots, b_{\ell'}$ are undetermined real constants such that [23, §31]

$$a_k = \frac{1}{2\pi} \int_{\Gamma_k} \frac{\partial u}{\partial \mathbf{n}} ds, \quad k = 1, 2, \ldots, m', \tag{6}$$

and

$$b_k = \frac{1}{2\pi} \int_{\Gamma_{m+k}} \frac{\partial u}{\partial \mathbf{n}} ds, \quad k = 1, 2, \ldots, \ell'.$$

Hence, using (4b), we have $b_k = 0$ for all $k = 1, 2, \ldots, \ell'$. Thus, the function F has the representation

$$F(z) = g(z) - \sum_{k=1}^{m'} a_k \log(z - \alpha_k). \tag{7}$$

Since u is harmonic in the domain G, then by Green's theorem (see [4, p. 4] and [13, p. 441]),

$$\int_{\Gamma} \frac{\partial u}{\partial \mathbf{n}} ds = 0,$$

which in view of (4b) implies that

$$\sum_{k=1}^{m} \int_{\Gamma_k} \frac{\partial u}{\partial \mathbf{n}} ds = 0. \tag{8}$$

Recall that $a_1, \ldots, a_{m'}$ are given in (6). So, if $m' = m - 1$, we define

$$a_m = \frac{1}{2\pi} \int_{\Gamma_m} \frac{\partial u}{\partial \mathbf{n}} ds. \tag{9}$$

Hence, it follows from (6), (8), and (9) that

$$\sum_{k=1}^{m} a_k = \sum_{k=1}^{m} \frac{1}{2\pi} \int_{\Gamma_k} \frac{\partial u}{\partial \mathbf{n}} ds = 0, \tag{10}$$

which implies, in the case $m' = m - 1$, that

$$a_m = -\sum_{k=1}^{m-1} a_k. \tag{11}$$

Using Green's formula [4, p. 4], Eq. (1) can be written as

$$\mathrm{cap}(C) = \int_{\partial G} u \frac{\partial u}{\partial \mathbf{n}} ds. \tag{12}$$

Since $\partial u/\partial \mathbf{n} = 0$ on $\partial B = \cup_{k=1}^{\ell} \Gamma_{m+k}$ and $u = \delta_k$ on Γ_k for $k = 1, 2, \ldots, m$, then in view of (6) and (9), we have

$$\mathrm{cap}(C) = \sum_{k=1}^{m} \delta_k \int_{\Gamma_k} \frac{\partial u}{\partial \mathbf{n}} ds = 2\pi \sum_{k=1}^{m} \delta_k a_k. \tag{13}$$

Eq. (13) gives us a simple formula for computing the capacity of the generalized condenser C in terms of the levels δ_k of the potential of the plates and the values of the constants a_k for $k = 1, 2, \ldots, m$.

In this paper, the boundary integral equation with the generalized Neumann kernel will be used to compute the constants a_k as well as the values of the function $u(z)$ for $z \in G$. However, to use the integral equation, we will first reformulate the above mixed boundary value problem as a Riemann–Hilbert problem as it will be described in the next section. Solving the mixed boundary value problem by reducing it to a Riemann–Hilbert problem is a well known approach and has been used by many researchers in the literature (see e.g., [25–29]).

3. The Riemann–Hilbert problem

For each $k = 1, 2, \ldots, m+\ell$, the boundary component Γ_k is parametrized by a 2π-periodic complex function $\eta_k(t)$, $t \in J_k := [0, 2\pi]$. The total parameter domain J is the disjoint union of the $m+\ell$ intervals $J_1, \ldots, J_{m+\ell}$,

$$J = \bigsqcup_{k=1}^{m+\ell} J_k = \bigcup_{k=1}^{m+\ell} \{(t,k) \ : \ t \in J_k\}.$$

The elements of J are ordered pairs (t,k) where k is an auxiliary index indicating which of the intervals contains the point t [21]. A parametrization of the whole boundary Γ is then defined by

$$\eta(t,k) = \eta_k(t), \quad t \in J_k, \quad k = 1, 2, \ldots, m+\ell. \tag{14}$$

For a given t, the value of an auxiliary index k such that $t \in J_k$ will be always clear from the context. So we replace the pair (t,k) on the left-hand side of (14) by t in the same way as in [21]. Thus, the function η in (14) is written as

$$\eta(t) = \begin{cases} \eta_1(t), & t \in J_1, \\ \eta_2(t), & t \in J_2, \\ \quad \vdots & \\ \eta_{m+\ell}(t), & t \in J_{m+\ell}. \end{cases} \tag{15}$$

The parametrization is compatible with the orientation of each boundary component described in Section 2.

Since $u = \delta_k$ is known on the boundary components Γ_k for $k = 1, 2, \ldots, m$ and since $u = \operatorname{Re} F$, then the boundary values of the function F satisfy

$$\operatorname{Re}[F(\eta(t))] = \delta_k, \quad \eta(t) \in \Gamma_k, \quad k = 1, 2, \ldots, m. \tag{16}$$

On the boundaries $\partial B = \cup_{k=1}^{\ell} \Gamma_{m+k}$, the potential function u satisfies the boundary condition $\partial u/\partial \mathbf{n} = 0$ where $\mathbf{n}$ is the outward normal vector on ∂B. Let $\mathbf{T}$ be the unit tangent vector on ∂B. Then, for $\eta(t) \in \partial B$,

$$\mathbf{n}(\eta(t)) = -\mathrm{i}\mathbf{T}(\eta(t)) = -\mathrm{i}\frac{\eta'(t)}{|\eta'(t)|} = e^{\mathrm{i}\nu(\eta(t))} \tag{17}$$

where $\nu(\eta(t))$ is the angle between the positive real axis and the normal vector $\mathbf{n}(\eta(t))$. Using the Cauchy–Riemann equations, the derivative of the analytic function F is then $F'(z) = \frac{\partial u(z)}{\partial x} - \mathrm{i}\frac{\partial u(z)}{\partial y}$. Thus,

$$\frac{\partial u}{\partial \mathbf{n}} = \nabla u \cdot \mathbf{n} = \cos(\nu)\frac{\partial u}{\partial x} + \sin(\nu)\frac{\partial u}{\partial y} = \operatorname{Re}\left[e^{\mathrm{i}\nu}\left(\frac{\partial u}{\partial x} - \mathrm{i}\frac{\partial u}{\partial y}\right)\right] = \operatorname{Re}\left[\frac{-\mathrm{i}\eta'(t)}{|\eta'(t)|}F'(\eta(t))\right] \tag{18}$$

which, in view of (4b), implies that

$$\operatorname{Re}\left[-\mathrm{i}\eta'(t)F'(\eta(t))\right] = 0, \quad \eta(t) \in \Gamma_{m+k}, \quad k = 1, 2, \ldots, \ell.$$

Integrating with respect to the parameter t yields

$$\operatorname{Re}[-\mathrm{i}F(\eta(t))] = \nu_k, \quad \eta(t) \in \Gamma_{m+k}, \quad k = 1, 2, \ldots, \ell, \tag{19}$$

where $\nu_1, \nu_2, \ldots, \nu_\ell$ are real constants of integration. Thus, by (16) and (19), the boundary values of the function F satisfy the boundary condition

$$\operatorname{Re}\left[e^{-\mathrm{i}\theta(t)}F(\eta(t))\right] = \delta(t) + \nu(t)$$

where

$$\theta(t) = \begin{cases} 0, & t \in J_1, \\ \quad \vdots & \\ 0, & t \in J_m, \\ \pi/2, & t \in J_{m+1}, \\ \quad \vdots & \\ \pi/2, & t \in J_{m+\ell}, \end{cases} \quad \delta(t) = \begin{cases} \delta_1, & t \in J_1, \\ \quad \vdots & \\ \delta_m, & t \in J_m, \\ 0, & t \in J_{m+1}, \\ \quad \vdots & \\ 0, & t \in J_{m+\ell}, \end{cases} \quad \nu(t) = \begin{cases} 0, & t \in J_1, \\ \quad \vdots & \\ 0, & t \in J_m, \\ \nu_1, & t \in J_{m+1}, \\ \quad \vdots & \\ \nu_\ell, & t \in J_{m+\ell}, \end{cases} \tag{20}$$

i.e., $\theta(t) = 0$ and $\nu(t) = 0$ for $\ell = 0$. Then, it follows from (7) that the single-valued analytic function g satisfies the boundary condition

$$\text{Re}\left[e^{-i\theta(t)}g(\eta(t))\right] = \delta(t) + \nu(t) + \sum_{k=1}^{m'} a_k \text{Re}\left[e^{-i\theta(t)}\log(\eta(t) - \alpha_k)\right]. \tag{21}$$

Lemma 1. *The functions γ_k, for $k = 1, \ldots, m'$, defined on J by*

$$\gamma_k(t) = \begin{cases} \text{Re}\left[e^{-i\theta(t)}\log(\eta(t) - \alpha_k)\right], & \text{if } \ell' = \ell, \\ \text{Re}\left[e^{-i\theta(t)}\log\dfrac{\eta(t) - \alpha_k}{\eta(t) - \alpha}\right], & \text{if } \ell' = \ell - 1, \end{cases} \tag{22}$$

are periodic for $t \in J_j$, $j = 1, 2, \ldots, m + \ell$. For both cases, we have

$$\sum_{k=1}^{m'} a_k\gamma_k(t) = \sum_{k=1}^{m'} a_k \text{Re}\left[e^{-i\theta(t)}\log(\eta(t) - \alpha_k)\right]. \tag{23}$$

Proof. Since $\theta(t) = 0$ when $t \in J_j$ for each $j = 1, 2, \ldots, m$, then the functions $\gamma_k(t)$ in (22) are periodic for $t \in J_j$ for each $j = 1, 2, \ldots, m$.

When $t \in J_j$ for each $j = m + 1, m + 2, \ldots, m + \ell$, we have the following two cases:

(a) $\ell' = \ell$. For this case, $\Gamma_{m+\ell}$ is not the external boundary component of G. Recall that, for each $k = 1, 2, \ldots, m'$, α_k is in the interior of the curve Γ_k. Thus, none of the auxiliary points $\alpha_1, \ldots, \alpha_{m'}$ is interior to any of the curves $\Gamma_{m+1}, \ldots, \Gamma_{m+\ell}$. Hence, the winding number of the function $z - \alpha_k$ is always zero along each boundary component Γ_{m+k} for $k = 1, 2, \ldots, \ell$. Thus, we can always choose a branch cut of the logarithm function such that the functions $\gamma_k(t)$ given by the first formula in (22) are periodic for $t \in J_j$ for each $j = m + 1, m + 2, \ldots, m + \ell$.

(b) $\ell' = \ell - 1$. For this case, $\Gamma_{m+\ell}$ is the external boundary component of G. Hence, none of the auxiliary points $\alpha, \alpha_1, \ldots, \alpha_{m'}$ is interior to any of the curves $\Gamma_{m+1}, \ldots, \Gamma_{m+\ell-1}$. However, all the auxiliary points $\alpha, \alpha_1, \ldots, \alpha_{m'}$ are interior to the curve $\Gamma_{m+\ell}$. Thus, the winding number of the function $\frac{z-\alpha_k}{z-\alpha}$ is always zero along each boundary component Γ_{m+k} for $k = 1, 2, \ldots, \ell$. Hence, we can choose a branch cut of the logarithm function such that the functions $\gamma_k(t)$ given by the second formula in (22) are periodic for $t \in J_j$ for each $j = m + 1, m + 2, \ldots, m + \ell$. For this case, we need to prove also that Eq. (23) holds for the functions $\gamma_k(t)$ defined by the second formula in (22). Since $\Gamma_{m+\ell}$ is the external boundary component of G, we have $m' = m$, and by (10), we have $\sum_{k=1}^{m'} a_k = 0$. Thus,

$$\begin{aligned} \sum_{k=1}^{m'} a_k\gamma_k(t) &= \sum_{k=1}^{m'} a_k \text{Re}\left[e^{-i\theta(t)}\log\frac{\eta(t) - \alpha_k}{\eta(t) - \alpha}\right] \\ &= \text{Re}\left[e^{-i\theta(t)}\log(\eta(t) - \alpha)\right]\sum_{k=1}^{m'} a_k + \sum_{k=1}^{m'} a_k \text{Re}\left[e^{-i\theta(t)}\log\frac{\eta(t) - \alpha_k}{\eta(t) - \alpha}\right] \\ &= \sum_{k=1}^{m'} a_k \text{Re}\left[e^{-i\theta(t)}\log(\eta(t) - \alpha) + e^{-i\theta(t)}\log\frac{\eta(t) - \alpha_k}{\eta(t) - \alpha}\right] \\ &= \sum_{k=1}^{m'} a_k \text{Re}\left[e^{-i\theta(t)}\log(\eta(t) - \alpha_k)\right], \end{aligned}$$

and hence (23) holds for the functions $\gamma_k(t)$ defined by the second formula in (22). □

Taking into account (23), we rewrite the boundary condition (21) as

$$\text{Re}\left[e^{-i\theta(t)}g(\eta(t))\right] = \delta(t) + \nu(t) + \sum_{k=1}^{m'} a_k\gamma_k(t) \tag{24}$$

where the functions γ_k are defined by (22). Since we are interested in computing only $u = \text{Re}\, F$, we can assume that $g(\infty) = c$ is real for unbounded G and $g(\alpha) = c$ is real for bounded G. We introduce an auxiliary function f defined in G by

$$f(z) = \begin{cases} g(z) - c, & \text{if } G \text{ is unbounded}, \\ (g(z) - c)/(z - \alpha), & \text{if } G \text{ is bounded}. \end{cases} \tag{25}$$

Then f is a single-valued analytic function in G with $f(\infty) = 0$ for unbounded G. Let $A(t)$ be the complex-valued function defined by [21]

$$A(t) = \begin{cases} e^{-i\theta(t)}, & \text{if } G \text{ is unbounded,} \\ e^{-i\theta(t)}(\eta(t) - \alpha), & \text{if } G \text{ is bounded.} \end{cases} \tag{26}$$

Hence the boundary condition (24) implies that the function f is a solution of the following Riemann–Hilbert problem

$$\text{Re } [A(t)f(\eta(t))] = -c\cos\theta(t) + \delta(t) + \nu(t) + \sum_{k=1}^{m'} a_k\gamma_k(t). \tag{27}$$

Observe that solving the Riemann–Hilbert problem (27) requires finding the unknown analytic functions f as well as the unknown real constants $a_1, \ldots, a_m, c, \nu_1, \ldots, \nu_\ell$ on the right-hand side of (27).

4. The generalized Neumann kernel

The generalized Neumann kernel $N(s, t)$ is defined for $(s, t) \in J \times J$ by [22]

$$N(s, t) = \frac{1}{\pi}\text{Im}\left(\frac{A(s)}{A(t)}\frac{\dot\eta(t)}{\eta(t) - \eta(s)}\right).$$

Closely related to the kernel N is the following kernel $M(s, t)$ defined for $(s, t) \in J \times J$ by [22]

$$M(s, t) = \frac{1}{\pi}\text{Re}\left(\frac{A(s)}{A(t)}\frac{\dot\eta(t)}{\eta(t) - \eta(s)}\right).$$

The kernel N is continuous and the kernel M is singular where the singular part of M involves the cotangent function [22].

Let H denote the space of all real-valued Hölder continuous functions on the boundary Γ. In this paper, for simplicity, if ϕ is a real-valued function defined on the boundary Γ, then we write $\phi(\eta(t))$ as $\phi(t)$. Further, we say that a function $h \in H$ is piecewise constant if for each $k = 1, \ldots, m + \ell$ there is a real number c_k such that

$$h(t) = c_k \quad \text{for} \quad t \in J_k.$$

Such a function will be denoted by

$$h(t) = (c_1, \ldots, c_{m+\ell}), \quad t \in J.$$

The integral operators with the kernels $N(s, t)$ and $M(s, t)$ are defined on H by

$$(\mathbf{N}\phi)(s) = \int_J N(s, t)\phi(t)\, dt, \quad s \in J, \tag{28}$$

$$(\mathbf{M}\phi)(s) = \int_J M(s, t)\phi(t)\, dt, \quad s \in J. \tag{29}$$

The identity operator on H will be denoted by $\mathbf{I}$.

For a given function $\gamma \in H$, by a solution of the Riemann–Hilbert problem

$$\text{Re}\,[A(t)f(\eta(t))] = \gamma(t), \tag{30}$$

we mean a function f analytic in G with $f(\infty) = 0$ for unbounded G, continuous on the closure $\overline{G}$, such that the boundary values of f satisfy on Γ the boundary condition (30). The solvability of the Riemann–Hilbert problem (30) depends on the index of the function A [27,28,30,31]. The index κ_j of the function A on the curve Γ_j is defined as the change of the argument of A along the curve Γ_j divided by 2π, i.e.,

$$\kappa_j = \frac{1}{2\pi}\Delta \arg(A)|_{\Gamma_j}, \quad j = 1, 2, \ldots, m + \ell.$$

The index κ of the function A on the whole boundary curve Γ is the sum $\kappa = \sum_{j=1}^{m+\ell} \kappa_j$.

For the function A defined in (26), if G is unbounded, the index of the function A is given by

$$\kappa_j = 0 \quad \text{for } j = 1, 2, \ldots, m + \ell,$$

and hence $\kappa = 0$. When G is bounded, then the external boundary component of G is either Γ_m or $\Gamma_{m+\ell}$. Define $\hat m = m$ if the external boundary component of G is Γ_m and $\hat m = m + \ell$ if the external boundary component of G is $\Gamma_{m+\ell}$. Then, the index of the function A in (26) is given by

$$\kappa_{\hat m} = 1, \quad \kappa_j = 0 \quad \text{if } j \neq \hat m \text{ for } j = 1, 2, \ldots, m + \ell,$$

and thus $\kappa = 1$. Hence, it follows from [22, Theorem 9] and [32, Theorem 4] that the Riemann–Hilbert problem (30) is not necessarily solvable. However, if the problem is solvable, then its solution is unique.

For bounded G, although the function A defined in (26) above is slightly different from the function A defined in [33, Eq. (13)], both functions have the same index. Similarly, for unbounded G, the function A in (26) has the same index as the function A given in [32, Eq. (62)]. Hence, the following two theorems can be proved for bounded G using the same approach used in [33] and for unbounded G using the same approach used in [32].

Theorem 1. *For a given function $\gamma \in H$, there exists a unique piecewise constant function $h = (c_1, \ldots, c_{m+\ell})$ such that the Riemann–Hilbert problem*

$$\operatorname{Re}[A(t)f(\eta(t))] = \gamma(t) + h(t) \tag{31}$$

is solvable and has a unique solution.

Proof. For bounded G, the proof is similar to the proof of Lemma 1 and Eq. (26) in [33].

For unbounded G, the proof is similar to the proof of Corollary 2, Eq. 64 and Eq. 67 in [32].

The uniqueness of the solution follows from [22, Theorem 9] for bounded G and from [32, Theorem 4] for unbounded G. □

The above theorem states that a unique piecewise constant function $h = (c_1, \ldots, c_{m+\ell})$ always exists such that adding this function h to the right-hand side of the problem (30) makes the problem solvable. This means modifying the right-hand side of the Riemann–Hilbert problem (30) by adding a suitable constant c_j to the values of the function γ for each of the boundary component Γ_j for $j = 1, 2, \ldots, m + \ell$. The real constants $c_1, \ldots, c_{m+\ell}$ are undetermined and need to be determined alongside the solution of the Riemann–Hilbert problem. This is analogous to the case of the modified Dirichlet problem as in [23, p. 150, Eq. (1)], [27, p. 327, Eq. (36.2)] and [28, p. 164, Eq. (60.2)].

We can conclude from Theorem 1 that for each of the functions γ_k given by (22), there exists a unique piecewise constant function h_k such that the Riemann–Hilbert problem

$$\operatorname{Re}[A(t)f_k(\eta(t))] = \gamma_k(t) + h_k(t) \tag{32}$$

is solvable, $k = 1, 2, \ldots, m'$. A method for computing the unknown function h_k as well as the boundary values of the solution f_k of the Riemann–Hilbert problem (32) is given in the following theorem (see also [34, Theorem 1]).

Theorem 2. *For each $k = 1, 2, \ldots, m'$, let the function γ_k be given by (22). Then, there exists a unique real-valued function $\mu_k \in H$ and a unique piecewise constant real-valued function $h_k = (h_{1,k}, h_{2,k}, \ldots, h_{m+\ell,k})$ such that*

$$A(t)f_k(\eta(t)) = \gamma_k(t) + h_k(t) + \mathrm{i}\mu_k(t), \quad t \in J, \tag{33}$$

are boundary values of an analytic function f_k in G with $f(\infty) = 0$ for unbounded G. The function μ_k is the unique solution of the integral equation

$$(\mathbf{I} - \mathbf{N})\mu_k = -\mathbf{M}\gamma_k \tag{34}$$

and the function h_k is given by

$$h_k = [\mathbf{M}\mu_k - (\mathbf{I} - \mathbf{N})\gamma_k]/2. \tag{35}$$

Proof. For bounded G, the proof is similar to the proof of Theorem 2 and Eq. (26) in [33].

For unbounded G, the proof is similar to the proof of Theorem 9 in [32]. □

The following lemma is needed to prove Theorems 3 and 4.

Lemma 2. *If f is an analytic function in G with $f(\infty) = 0$ for unbounded G such that its boundary values satisfy the boundary condition*

$$\operatorname{Re}[A(t)f(\eta(t))] = \gamma(t) \tag{36}$$

for a piecewise constant real-valued function $\gamma(t) = (c_1, c_2, \ldots, c_{m+\ell})$, then f is the zero function and $c_1 = c_2 = \cdots = c_{m+\ell} = 0$.

Proof. By Theorem 1, a unique piecewise constant real-valued function $h(t) = (c_1, c_2, \ldots, c_{m+\ell})$ exists such that the Riemann–Hilbert problem

$$\operatorname{Re}[A(t)f(\eta(t))] = \gamma(t) + h(t)$$

is uniquely solvable. By the uniqueness of the piecewise constant function h and since the function γ is a piecewise constant function, the function h must be given by $h(t) = -\gamma(t)$ since the problem

$$\operatorname{Re}[A(t)f(\eta(t))] = \gamma(t) + h(t) = 0$$

will be solvable and has the zero solution $f(z) = 0$. Thus, γ is the zero function and hence $c_1 = c_2 = \cdots = c_{m+\ell} = 0$. □

5. The numerical method

In this section, we shall use Theorem 2 to present a method for computing the real constants $a_1, \ldots, a_m$ and hence computing cap(C) through (13). Recall from (2) that either $m' = m$ or $m' = m-1$. These two cases of m' will be considered separately in the following two subsections.

5.1. Case I: $m' = m$

This case includes the following two subcases:

1. Both G and B are unbounded (see Fig. 1). For this subcase, we have $m' = m \geq 2$, $\ell' = \ell \geq 0$ (where $B = \mathbb{C}$ for $\ell = 0$), A is given by the first formula in (26), and the functions γ_k for $k = 1, 2, \ldots, m$ are given by the first formula in (22).
2. Both G and B are bounded (see Fig. 2). For this subcase, we have $m' = m \geq 2$, $\ell' = \ell - 1 \geq 0$, $\Gamma_{m+\ell}$ is the external boundary component of G, A is given by the second formula in (26), and the functions γ_k for $k = 1, 2, \ldots, m$ are given by the second formula in (22).

For these two subcases, all the simply connected domains $G_1, \ldots, G_m$ are bounded (see Figures 1 and 2). In Fig. 1 and 2, and in all figures throughout the paper, the boundaries of the domain B are the "dash-dotted" curves and the boundaries of the plates of the condenser are the "solid" curves.

The following theorem provides us with a method for computing the unknown real constants $a_1, \ldots, a_m$. The theorem will be proved using an approach similar to the approach used in proving Theorems 4.2 and 4.3 in [35],

Theorem 3. *For each $k = 1, 2, \ldots, m$, let the function γ_k be defined by (22), μ_k be the unique solution of the integral equation (34), and the piecewise constant function $h_k = (h_{1,k}, h_{2,k}, \ldots, h_{m+\ell,k})$ be given by (35). Then, the boundary values of the function f in (27) are given by*

$$A(t)f(\eta(t)) = \sum_{k=1}^{m} a_k[\gamma_k(t) + h_k(t) + \mathrm{i}\mu_k(t)] \tag{37}$$

and the $m + \ell + 1$ unknown real constants $a_1, \ldots, a_m, c, \nu_1, \ldots, \nu_\ell$ are the components of the unique solution vector of the linear system

$$\left[\begin{array}{ccc|c|ccc} h_{1,1} & \cdots & h_{1,m} & 1 & & & \\ \vdots & \ddots & \vdots & \vdots & & \boldsymbol{O} & \\ h_{m,1} & \cdots & h_{m,m} & 1 & & & \\ \hline h_{m+1,1} & \cdots & h_{m+1,m} & 0 & -1 & & \\ \vdots & \ddots & \vdots & \vdots & & \boldsymbol{O} & \\ h_{m+\ell,1} & \cdots & h_{m+\ell,m} & 0 & 0 & \cdots & -1 \\ \hline 1 & \cdots & 1 & 0 & 0 & \cdots & 0 \end{array}\right] \left[\begin{array}{c} a_1 \\ \vdots \\ a_m \\ \hline c \\ \hline \nu_1 \\ \vdots \\ \nu_\ell \end{array}\right] = \left[\begin{array}{c} \delta_1 \\ \vdots \\ \delta_m \\ 0 \\ \vdots \\ 0 \\ \hline 0 \end{array}\right]. \tag{38}$$

Proof. Suppose that f is the analytic function in G with $f(\infty) = 0$ for unbounded G and satisfies the boundary condition (27). Suppose also that $\hat{f}$ is defined in G by

$$\hat{f}(z) = \sum_{k=1}^{m} a_k f_k(z) \tag{39}$$

where f_k are as in Theorem 2 and the constants $a_1, \ldots, a_m$ satisfy the condition (10). Then $\hat{f}$ is analytic in G with $f(\infty) = 0$ for unbounded G and the boundary values of $\hat{f}$ satisfy

$$\mathrm{Re}\left[A(t)\hat{f}(\eta(t))\right] = \sum_{k=1}^{m} a_k\gamma_k(t) + \sum_{k=1}^{m} a_k h_k(t). \tag{40}$$

Then the function Ψ defined by $\Psi(z) = \hat{f}(z) - f(z)$ is analytic in G with $\Psi(\infty) = 0$ for unbounded G. Since $m' = m$, it follows from (27) and (40) that

$$\mathrm{Re}\,[A(t)\Psi(\eta(t))] = \sum_{k=1}^{m} a_k h_k(t) + c\cos\theta(t) - \delta(t) - \nu(t). \tag{41}$$

The right-hand side is a piecewise constant function, and then Lemma 2 implies that Ψ is the zero function and hence $f(z) = \hat{f}(z)$. Thus, (37) follows from (33) and (39). Further, since Ψ is the zero function, the right-hand side of (41) is also

the zero function and hence

$$\sum_{k=1}^{m} a_k h_k + c\cos\theta(t) - \nu(t) = \delta(t). \tag{42}$$

Since, in view of (20), $\cos\theta(t) = 1$ for $t \in J_k$ for $k = 1, 2, \ldots, m$ and $\cos\theta(t) = 0$ for $t \in J_k$ for $k = m+1, m+2, \ldots, m+\ell$, then (42) and (10) imply that the real constants $a_1, \ldots, a_m, c, \nu_1, \ldots, \nu_\ell$ are the components of a solution vector of the linear system (38).

To show that the linear system (38) has a unique solution, let $[a_1, \ldots, a_m, c, \nu_1, \ldots, \nu_\ell]^T$ be a solution to the homogeneous linear system obtained by assuming that the right-hand side of (38) is the zero vector. Then, the homogeneous system implies that

$$\sum_{k=1}^{m} a_k h_k + c\cos\theta(t) - \nu(t) = 0, \quad \sum_{k=1}^{m} a_k = 0. \tag{43}$$

Assume that the functions f_k are as in Theorem 2 and $\hat{f}$ is defined by (39). Hence, in view of (40), the boundary values of the function $\hat{f}$ satisfy

$$\mathrm{Re}\left[A(t)\hat{f}(\eta(t))\right] = \sum_{k=1}^{m} a_k \gamma_k(t) + \nu(t) - c\cos\theta(t). \tag{44}$$

Then, we define a function $\hat{F}$ in G by

$$\hat{F}(z) = \begin{cases} (z-\alpha)\hat{f}(z) - \displaystyle\sum_{k=1}^{m} a_k \log(z-\alpha_k), & \text{if } G \text{ is bounded,} \\ \hat{f}(z) - \displaystyle\sum_{k=1}^{m} a_k \log(z-\alpha_k), & \text{if } G \text{ is unbounded,} \end{cases} \tag{45}$$

For unbounded G, the function $\hat{F}(z)$ can be written as

$$\hat{F}(z) = \hat{f}(z) - \sum_{k=1}^{m} a_k[\log z + \log(1-\alpha_k/z)] = \hat{f}(z) - \log z \sum_{k=1}^{m} a_k - \sum_{k=1}^{m} a_k \log(1-\alpha_k/z).$$

Since $\hat{f}(\infty) = 0$ and $\sum_{k=1}^{m} a_k = 0$, we have $\hat{F}(\infty) = 0$. Thus, the function $\hat{F}(z)$ is analytic in G for both cases of bounded and unbounded G but it is not necessarily single valued. In view of (26), the boundary values of the function $\hat{F}$ satisfy

$$\mathrm{Re}\left[e^{-\mathrm{i}\theta(t)}\hat{F}(\eta(t))\right] = \mathrm{Re}\left[A(t)\hat{f}(\eta(t))\right] - \sum_{k=1}^{m} a_k \mathrm{Re}\left[e^{-\mathrm{i}\theta(t)}\log(\eta(t)-\alpha_k)\right].$$

Then by (23) and (44), we have

$$\mathrm{Re}\left[e^{-\mathrm{i}\theta(t)}\hat{F}(\eta(t))\right] = \nu(t) - c\cos\theta(t),$$

which, in view of (20), implies that

$$\mathrm{Re}\left[\hat{F}(\eta(t))\right] = -c \quad \text{for} \quad \eta(t) \in \Gamma_k,\ k = 1, 2, \ldots, m, \tag{46a}$$

and

$$\mathrm{Im}\left[\hat{F}(\eta(t))\right] = \nu_k \quad \text{for} \quad \eta(t) \in \Gamma_k,\ k = m+1, m+2, \ldots, m+\ell. \tag{46b}$$

Differentiating both sides of (46b) with respect to the parameter t, we obtain

$$\mathrm{Im}\left[\eta'(t)\hat{F}'(\eta(t))\right] = 0 \quad \text{for} \quad \eta(t) \in \Gamma_k,\ k = m+1, m+2, \ldots, m+\ell. \tag{47}$$

Let the real function u be defined for $z \in G \cup \partial G$ by

$$u(z) = \mathrm{Re}\,\hat{F}(z).$$

Then u is harmonic in G. In view of (18), we have

$$\frac{\partial u}{\partial \mathbf{n}} = \mathrm{Re}\left[\frac{-\mathrm{i}\eta'(t)}{|\eta'(t)|}\hat{F}'(\eta(t))\right] = \frac{1}{|\eta'(t)|}\mathrm{Im}\left[\eta'(t)\hat{F}'(\eta(t))\right]. \tag{48}$$

Thus, by (46a), (47), and (48), the boundary values of u satisfy the mixed-boundary condition

$$u(\zeta) = -c, \quad \zeta \in \Gamma_k, \quad k = 1, 2, \ldots, m,$$
$$\frac{\partial u}{\partial \mathbf{n}}(\zeta) = 0, \quad \zeta \in \Gamma_k, \quad k = m+1, m+2, \ldots, m+\ell.$$

Since the above mixed boundary value problem has a unique solution, it is clear that the unique solution is the constant function $u(z) = -c$ for all $z \in G \cup \partial G$. Thus the real part of $\hat{F}$ is constant for $z \in G$, and hence, by the Cauchy–Riemann equations, $\hat{F}$ is constant in G, say equal to C. This implies that $\hat{F}(z) = 0$ for all $z \in G$ when G is unbounded since $\hat{F}(\infty) = 0$. Then, for all $z \in G$, it follows from (45) that

$$\sum_{k=1}^{m} a_k \log(z - \alpha_k) = \begin{cases} -C + (z-\alpha)\hat{f}(z), & \text{if } G \text{ is bounded,} \\ \hat{f}(z), & \text{if } G \text{ is unbounded,} \end{cases}$$

which implies that $a_1 = a_2 = \cdots = a_m = 0$ since the functions on the right-hand side are single-valued and the function on the left-hand side is multi-valued. Thus, for bounded G, we have $(z-\alpha)\hat{f}(z) = C$ for all $z \in G$. By substituting $z = \alpha$, we find $C = 0$ and hence $\hat{F}(z) = 0$ for all $z \in G \cup \partial G$. Thus for both cases of bounded and unbounded G, we have $F(z) = 0$ for all $z \in G \cup \partial G$. Hence, it follows from (46) that $c = 0$ and $\nu_1 = \nu_2 = \cdots = \nu_\ell = 0$. Thus, the homogeneous linear system has only the trivial solution $[a_1, \ldots, a_m, c, \nu_1, \ldots, \nu_\ell]^T = \mathbf{0}$, and hence the matrix of the linear system (38) is non-singular. □

5.2. Case II: $m' = m - 1$

For this case, G is a bounded multiply connected domain of connectivity $m + \ell$ with $m \geq 2$ and B is an unbounded multiply connected domain of connectivity $\ell' = \ell \geq 0$ (where $B = \mathbb{C}$ for $\ell = 0$). Here, the simply connected domains $G_1, \ldots, G_{m-1}$ are bounded, the simply connected domain G_m is unbounded, and Γ_m is the external boundary component of G (see Fig. 3). Further, A is given by the second formula in (26) and the functions γ_k for $k = 1, 2, \ldots, m-1$ are given by the first formula in (22). For this case, the values of the unknown real constants $a_1, \ldots, a_{m-1}, c, \nu_1, \ldots, \nu_\ell$ can be computed as in the following theorem. Then a_m is computed through (11).

Theorem 4. *For each $k = 1, 2, \ldots, m-1$, let the function γ_k be defined by (22), let μ_k be the unique solution of the integral equation (34), and let the piecewise constant function $h_k = (h_{1,k}, h_{2,k}, \ldots, h_{m+\ell,k})$ be given by (35). Then, the boundary values of the function f in (27) are given by*

$$A(t) f(\eta(t)) = \sum_{k=1}^{m-1} a_k [\gamma_k(t) + h_k(t) + \mathrm{i}\mu_k(t)] \tag{49}$$

and the $m + \ell$ unknown real constants $a_1, \ldots, a_{m-1}, c, \nu_1, \ldots, \nu_\ell$ are the unique solution of the linear system

$$\left[\begin{array}{ccc:c:ccc} h_{1,1} & \cdots & h_{1,m-1} & 1 & & & \\ \vdots & \ddots & \vdots & \vdots & & \boldsymbol{O} & \\ h_{m,1} & \cdots & h_{m,m-1} & 1 & & & \\ \hdashline h_{m+1,1} & \cdots & h_{m+1,m-1} & 0 & -1 & & \boldsymbol{O} \\ \vdots & \ddots & \vdots & \vdots & & \ddots & \\ h_{m+\ell,1} & \cdots & h_{m+\ell,m-1} & 0 & \boldsymbol{O} & & -1 \end{array}\right] \left[\begin{array}{c} a_1 \\ \vdots \\ a_{m-1} \\ \hdashline c \\ \hdashline \nu_1 \\ \vdots \\ \nu_\ell \end{array}\right] = \left[\begin{array}{c} \delta_1 \\ \vdots \\ \delta_m \\ 0 \\ \vdots \\ 0 \end{array}\right]. \tag{50}$$

Proof. The theorem can be proved by the same argument as in the proof of Theorem 3. □

5.3. Computing the capacity cap(C) and the potential function u

By solving the integral equations (34) and then solving the linear system (38) (or (50)), we obtain the real constants $a_1, \ldots, a_m$. Then, we can compute the capacity $\mathrm{cap}(C)$ from (13). We can also compute the boundary values of the auxiliary analytic function $f(z)$ through (37) or (49). Then the values of $f(z)$ at interior points $z \in G$ can be computed by Cauchy's integral formula. Since $u(z) = \mathrm{Re}\,[F(z)]$, it follows from (7) and (25) that the function $u(z)$ is given for $z \in G$ by

$$u(z) = \begin{cases} c + \mathrm{Re}\,[(z-\alpha)f(z)] - \displaystyle\sum_{k=1}^{m'} a_k \log|z - \alpha_k|, & \text{if } G \text{ is bounded,} \\ c + \mathrm{Re}\,[f(z)] - \displaystyle\sum_{k=1}^{m'} a_k \log|z - \alpha_k|, & \text{if } G \text{ is unbounded,} \end{cases} \tag{51}$$

As it was pointed out in [15], the actual values of the auxiliary points α and α_j for $j = 1, 2, \ldots, m'$ are not important. Although the right-hand side of (51) involves these auxiliary points, several numerical experiments indicate that the values of the function u do not depend on the values of these auxiliary points as long as these points are sufficiently far away from the boundary of G.

5.4. Outline of the algorithm

The method presented in this section for computing the capacity $\text{cap}(C)$ and the potential function u can be summarized in the following algorithm. Steps 10–12 are needed only if it is required to compute the values of the potential function.

Algorithm 1. (Computing the capacity $\text{cap}(C)$ and the potential function u).

1. Parametrize the boundary components Γ_j by $\eta_j(t)$, $t \in [0, 2\pi]$, for $j = 1, 2, \ldots, m + \ell$, where Γ_j for $j = 1, 2, \ldots, m$ are the boundaries of the plates E_j of the condenser and Γ_j for $j = m+1, m+2, \ldots, m$ are the boundary components of the domain B.
2. If G is bounded and B is unbounded, then we define $m' = m - 1$ and $\ell' = \ell$. For this case, the plates $E_1, \ldots, E_{m-1}$ are bounded, the plate E_m is unbounded and Γ_m is the external boundary component of G.
3. If both domains B and G are bounded, then we define $m' = m$ and $\ell' = \ell - 1$. For this case, the plates $E_1, \ldots, E_m$ are bounded and $\Gamma_{m+\ell}$ is the external boundary component of G.
4. If both domains B and G are unbounded, then we define $m' = m$ and $\ell' = \ell$. For this case, the plates $E_1, \ldots, E_m$ are bounded.
5. Define the functions A by (26).
6. Define the functions γ_k for $k = 1, 2, \ldots, m'$ by (22).
7. For $k = 1, 2, \ldots, m'$, compute the function μ_k by solving the integral equation (34) and compute the function h_k through (35).
8. Compute the $m + \ell + 1$ real constants $a_1, \ldots, a_m, c, \nu_1, \ldots, \nu_\ell$ by solving one of the linear systems (38) or (50). For $m' = m - 1$, a_m is computed through (11).
9. Compute the capacity $\text{cap}(C)$ from (13).
10. Compute the boundary values of the analytic function f through (37) or (49).
11. Compute the values of $f(z)$ for $z \in G$ by the Cauchy integral formula.
12. Compute the values of the potential function u by (51).

6. Numerical implementation of the algorithm

The main steps in the Algorithm 1 are steps 7 and 8. In step 7, it is required to solve the integral equations with the generalized Neumann kernel (34) for m' different right-hand sides. The integral equation (34) has been used before in several publications, see e.g., [21,25,26,35–37]. So, we omit the details here about its numerical solution and refer the reader to [21] where a detailed numerical method for solving the integral equation (34) is presented. More importantly, an easy to use MATLAB function `fbie` for solving the integral equation (34) has been presented in [21]. Thus, in step 7 in Algorithm 1, the m' functions μ_k in (34) will be computed using the MATLAB function `fbie`. The function `fbie` computes also the m' piecewise constant functions h_k in (35). In the function `fbie`, the integral equation (34) is discretized by the Nyström method [38] with the trapezoidal rule [39,40]. The size of the obtained linear system is usually large. So, in the function `fbie`, the linear system is solved iteratively using the MATLAB function `gmres`. The matrix–vector multiplication in `gmres` is computed in a fast and efficient way using the MATLAB function `zfmm2dpart` from the toolbox `FMMLIB2D` [41].

For step 8 in Algorithm 1, in view of (38) and (50), the size of the matrix of the linear system is $(m+\ell+1)\times(m+\ell+1)$ if $m' = m$ and $(m + \ell) \times (m + \ell)$ if $m' = m - 1$. Thus, the size of the linear system is usually quite small and hence we solve it using MATLAB "backslash" operator.

The condition number of the matrix of the linear system in step 7 in Algorithm 1 is bounded and mostly independent of the size of the matrix [21,42]. For the condition number of the matrix of the linear system in step 8, Table 1 presents the condition number of the matrix for the examples presented in Section 7–10. The numerical results presented in Table 1, and other numerical results not reported here, show that the matrix of the linear system in step 8 is well conditioned but its condition number depends on the size of the matrix.

For domains with smooth boundaries, we use the trapezoidal rule with equidistant nodes. We discretize each interval $J_k = [0, 2\pi]$, for $k = 1, 2, \ldots, m + \ell$, by n equidistant nodes $s_1, \ldots, s_n$ where

$$s_k = (k-1)\frac{2\pi}{n}, \quad k = 1, \ldots, n, \tag{52}$$

and n is an even integer. We write $\mathbf{s} = [s_1, \ldots, s_n]$. Then, we discretize the parameter domain J by the $m + \ell$ copies of $\mathbf{s}$,

$$\mathbf{t} = [\mathbf{s}, \mathbf{s}, \ldots, \mathbf{s}]^T. \tag{53}$$

Table 1
The condition number of the matrix of the linear system in step 8 in Algorithm 1 for the examples in Sections 7–10.

Section	m	m′	ℓ	Size of the matrix	Condition number
7.1 ($a = 2, r = 0.5$)	2	2	0	3×3	2.15
7.2 ($a = 0.2, b = 0.7$)	3	2	0	3×3	3.58
7.3	16	16	0	17×17	13.56
	256	256	0	257×257	208.45
7.4	17	16	0	17×17	14.21
	257	256	0	257×257	225.75
8.1 (bounded, $r = 0.5$)	2	2	4	7×7	3.3589
(unbounded, $r = 0.5$)	2	2	4	7×7	28.669
8.2	5	4	0	5×5	10.65
8.3	2	1	72	74×74	221.12
	2	1	584	586×586	1405.60
	2	1	4680	4682×4682	8967.90
9.1 ($a = -0.5, b = 0.5, c = 2$)	3	3	0	4×4	1.72
9.2 ($a = -0.5, b = 0.5, c = 2$, $B = \mathbb{C}\backslash[a, b]$)	2	2	1	4×4	8.33
($a = -0.5, b = 0.5, c = 2$, $B = \mathbb{C}\backslash[a + \mathrm{i}, b + \mathrm{i}]$)	2	2	1	4×4	6.73
9.3	16	16	0	17×17	38.91
	256	256	0	257×257	600.02
9.4	4	3	0	4×4	6.97
10.1	2	1	0	2×2	2.41
10.2	4	3	0	4×4	8.84
10.3	16	16	0	17×17	9.31
	256	256	0	257×257	150.38
	1024	1024	0	1025×1025	601.84

This leads to the discretizations

$$\eta(\mathbf{t}) = [\eta_1(\mathbf{s}), \eta_2(\mathbf{s}), \ldots, \eta_{m+\ell}(\mathbf{s})]^T, \quad \eta'(\mathbf{t}), \quad A(\mathbf{t}), \quad \gamma_k(\mathbf{t}), \ k = 1, 2, \ldots, m'. \tag{54}$$

In MATLAB, these discretized functions are stored in the vectors `et`, `etp`, `A`, `gamk`, respectively. Then the discretizations vectors `muk` and `hk` of the functions μ_k and h_k in (34) and (35) are computed by calling

```
[muk,hk] = fbie(et,etp,A,gamk,n,iprec,restart,tol,maxit).
```

In the numerical experiments in the next sections, we choose `iprec` $= 5$ (the tolerance of the FMM is 0.5×10^{-15}), `restart=[]` (GMRES is used without restart), `tol=1e-14` (the tolerance of the GMRES method is 10^{-14}), and `maxit=100` (the maximum number of GMRES iterations is 100). The values $h_{j,k}$ are then computed by taking arithmetic means:

$$h_{j,k} = \frac{1}{n} \sum_{i=1+(j-1)n}^{jn} h_k(t_i), \quad j = 1, 2, \ldots, m + \ell, \quad k = 1, 2, \ldots, m'.$$

These values are used to build the linear system (38) or (50). Thus, the computational cost of the overall method for computing the capacity $\mathrm{cap}(C)$ is $O(m'(m + \ell)n \ln n)$ operations for step (7) and $O((m + \ell)^3)$ operations for step (8).

For fast and accurate computing of the Cauchy integral formula in step (11), we use the MATLAB function `fcau` from [21]. The function `fcau` is based on using the MATLAB function `zfmm2dpart` in [41]. Using the function `fcau`, the Cauchy integral formula can be computed at p interior points in $O(p + (m + \ell)n)$ operations.

For domains with corners (excluding cusps), the trapezoidal rule with equidistant nodes yields only poor convergence and hence the trapezoidal rule with a graded mesh will be used [43]. Equivalently, we can remove the discontinuity of the derivatives of the solution of the integral equation at the corner points by choosing an appropriate one-to-one function $\sigma : J \to J$. Then we parametrize the boundary Γ by $\eta(t) = \hat{\eta}(\sigma(t))$ where $\hat{\eta}$ is any parametrization function of the boundary Γ (see [15,43] for more details, the above function σ is denoted by δ in [15]).

The proposed method can be implemented in MATLAB as in the function `capgc.m` in Appendix. All the computer codes of our computations are available in the internet link: https://github.com/mmsnasser/gc.

In this paper, computations were performed in MATLAB R2017a on an ASUS Laptop with Intel(R) Core(TM) i7-8750H CPU @2.20 GHz, 2208 Mhz, 6 Core(s), 12 Logical Processor(s), and 16GB RAM. The computation times presented in this paper were measured with the MATLAB tic toc commands.

7. Numerical examples - classical condensers

In this section, we shall consider several numerical examples of condensers with $\ell = 0$ and $\{\delta_k\}_{k=1}^m$ containing exactly two different numbers which are 1 and 0 (see [4, p. 6] and [44, p. 202]). We shall call such condensers as *classical condensers*. Some of these examples either have known capacity or have been considered in the literature. So, we can compare the obtained results with the exact capacity or with known capacity computed by other researchers.

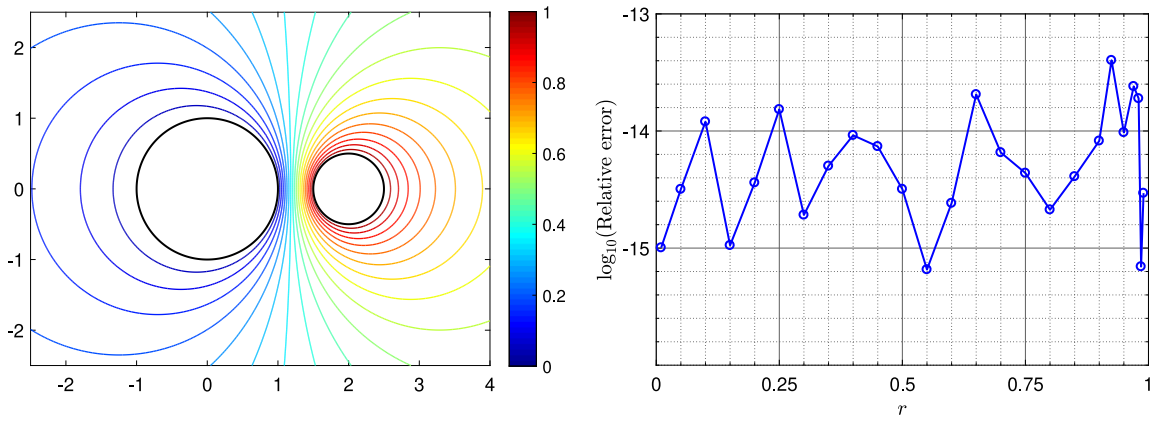

Fig. 4. The field of the condenser and the level curves of the function u for Section 7.1 (left) and the relative errors in the computed values (right).

7.1. Two circles

In this example, we consider the generalized condenser $C = (B, E, \delta)$ with $B = \mathbb{C}$ (and hence $\ell = 0$), $E = \{E_1, E_2\}$ (and hence $m = 2$), and $\delta = \{0, 1\}$. The plates of the condenser are given by $E_k = \overline{G_k}$, $k = 1, 2$, where $G_1 = \{z : |z| < 1\}$ and $G_2 = \{z : |z - a| < r\}$ for $r > 0$ and a real number a with $a > 1 + r$. So, for this example, the generalized condenser reduces to a classical condenser, $\ell' = \ell = 0$, and $m' = m = 2$. Thus, the field of the condenser, G is the doubly connected domain in the exterior of the two circles $\Gamma_1 = \{z : |z| = 1\}$ and $\Gamma_2 = \{z : |z - a| = r\}$ (see Fig. 4 (left) for $a = 2$ and $r = 0.5$). The exact value of the conformal capacity is given by $\mathrm{cap}(G) = 2\pi/\log(1/q)$ where q is obtained by solving the following equation [14]

$$\frac{(1+q)^2}{q} = \frac{(1+a-r)(a+r-1)}{r}.$$

We use the method presented in Section 6 with $n = 2^{10}$ to compute approximate values for the capacity for $a = 2$ and for several values of r between 0.01 and 0.99. The relative errors for the computed values for this case are presented in Fig. 4(right). The level curves of the function u for $a = 2$ and $r = 0.5$ are shown in Fig. 4 (left).

7.2. Square with two triangles

In this example, we consider the generalized condenser $C = (B, E, \delta)$ with $B = \mathbb{C}$, $E = \{E_1, E_2, E_3\}$ where $E_k = \overline{G_k}$, $k = 1, 2, 3$, and $\delta = \{1, 1, 0\}$. Here, G_1 is the interior of the triangles with the vertices ia, $-(b-a)/\sqrt{3}+ib$, $(b-a)/\sqrt{3}+ib$, G_2 is the interior of the triangles with the vertices $-ia$, $(b-a)/\sqrt{3}-ib$, $-(b-a)/\sqrt{3}-ib$, and G_3 is the exterior of the square with the vertices $1+i$, $-1+i$, $-1-i$, $1-i$. So, $\ell' = \ell = 0$, $m = 3$, $m' = 2$, and the generalized condenser reduces to a classical condenser. The field of the condenser, G, is then the bounded multiply connected domain in the exterior of the two triangles and in the interior of the square (see Fig. 5).

This example has been considered in [9, Example 7] for several values of a and b. We use the presented method with $n = 3 \times 2^{13}$ to compute the capacity for the same values of a and b used in [9]. The obtained results as well as the results presented in [9] are shown in Table 2. The level curves of the function u for $a = 0.2$ and $b = 0.7$ are shown in Fig. 5.

7.3. Cantor dust

Cantor dust is a generalization of the classical Cantor middle third set to dimension two. Let $I_0 = [0, 1]$ and recursively define

$$I_k = \frac{1}{3}I_{k-1} \cup \left(\frac{1}{3}I_{k-1} + \frac{2}{3}\right), \quad k \geq 1.$$

This means that I_k is constructed by "removing" the middle one third of each interval I_{k-1}. For $k = 0, 1, 2, \ldots$, the closed set I_k consists of 2^k closed intervals. Then, we define the closed sets S_k as

$$S_k = I_k \times I_k, \quad k \geq 0,$$

where S_k consists of 4^k closed square regions, say $E_1, E_2, \ldots, E_{4^k}$ (see Fig. 6 for $k = 1$ (left) and $k = 2$ (right)). Then the Cantor dust is defined as

$$S = \bigcap_{k=1}^{\infty} S_k.$$

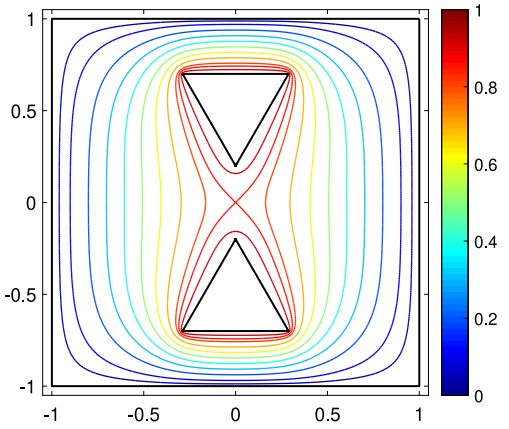

Fig. 5. The field of the condenser and the level curves of the function u for the condenser in Section 7.2.

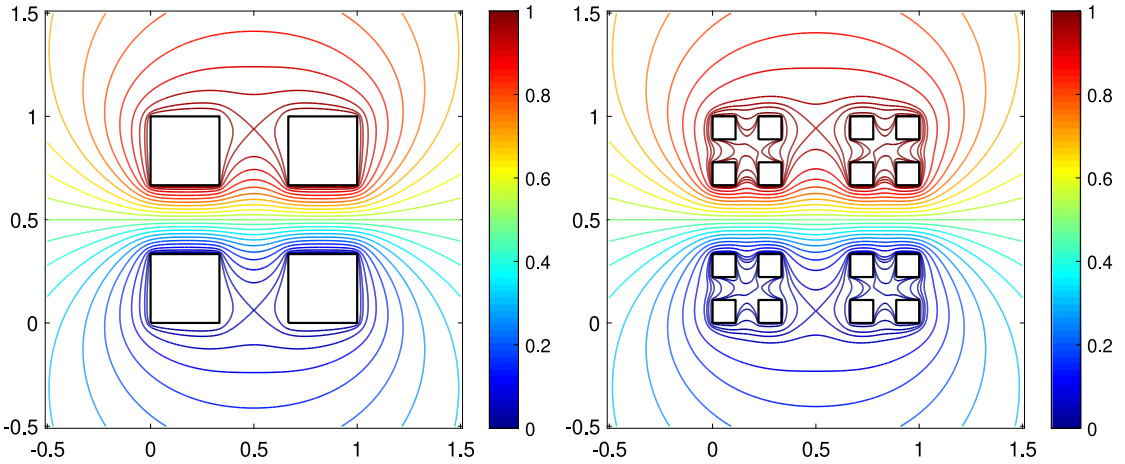

Fig. 6. The level curves of the function u for the condenser in Section 7.3 for $k = 1$ (left) and $k = 2$ (right).

Table 2
The approximate values of the capacity cap(C) for Section 7.2.

a	b	Our method	Betsakos et al. [9]
0.1	0.3	3.93241437137267	3.9324143
0.2	0.4	4.41198623240832	4.4119861
0.2	0.7	9.49308124679268	9.4930811
0.3	0.8	12.1180118821912	12.1180117
0.3	0.9	21.6586490491066	21.6586487

For $k = 0, 1, 2, \ldots$, we consider the generalized condensers $C_k = (B, E, \delta)$ with $B = \mathbb{C}$ and $E = \{E_1, E_2, \ldots, E_{4^k}\}$, i.e., we have 4^k plates. For the levels of the potential function $\delta = \{\delta_j\}_{j=1}^{4^k}$, we assume $\delta_j = 0$ for half of the plates (the plates below the line $y = 0.5$) and $\delta_j = 1$ for the other half (the plates above the line $y = 0.5$). Thus, $\ell = 0$, $m' = m = 4^k$, and the generalized condenser reduces to a classical condenser. The field of the condenser, G, is then the unbounded multiply connected domain in the exterior of the closed sets S_k (see Fig. 6).

The approximate value of the capacity for $k = 1, 2, 3, 4, 5$ are shown in Table 3 and the level curves of the function u for $k = 1, 2$ are shown in Fig. 6. For each k, the method requires solving $m' = 4^k$ integral equations. The CPU time presented in Table 3 shows that the method can be used to compute the capacity cap(C_k) in reasonable time even when m' becomes large. The presented method is used with $n = 2^9$.

Table 3
The approximate values of the capacity $\mathrm{cap}(C_k)$ for Section 7.3.

k	$m = 4^k$	$\mathrm{cap}(C_k)$	Time (sec)
1	4	4.652547172280	0.96
2	16	4.562140107251	7.33
3	64	4.531267950053	87.23
4	256	4.519885740453	1312.67
5	1024	4.515629401820	19880.56

Table 4
The approximate values of the capacity $\mathrm{cap}(C_k)$ for Section 7.4.

k	$m' = 4^k$	$\mathrm{cap}(C_k)$	Time (sec)
0	1	11.953050425798967	0.18
1	4	11.598538784854115	1.39
2	16	11.460679479701366	9.49
3	64	11.408998221761493	94.22
4	256	11.389646177509054	1235.45
5	1024	11.382387009959178	19160.17

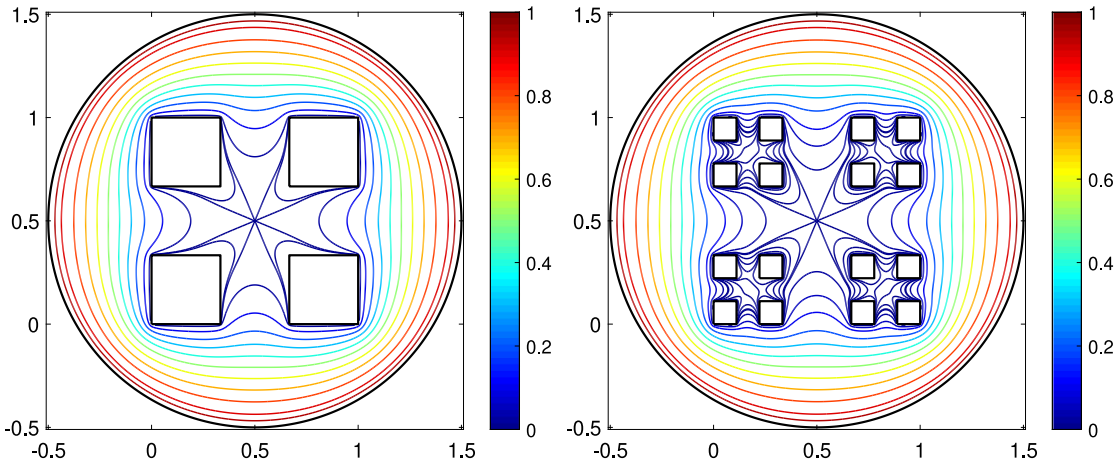

Fig. 7. The level curves of the function u for the condenser in Section 7.4 for $k = 1$ (left) and $k = 2$ (right).

7.4. Cantor dust in a circle

In this example, we consider the generalized condensers $C_k = (B, E, \delta)$ with $B = \mathbb{C}$, $E = \{E_1, E_2, \ldots, E_{4^k}, E_{4^k+1}\}$ where $E_1, E_2, \ldots, E_{4^k}$ are as in Section 7.3 and $E_{4^k+1} = \{z \in \mathbb{C} : |z - (0.5 + 0.5\mathrm{i})| \geq 1\}$. For the levels of the potential function, we assume $\delta = \{0, 0, \ldots, 0, 1\}$, i.e., the boundary values of the potential function u are 1 on the circle $|z - (0.5 + 0.5\mathrm{i})| = 1$ and 0 on the boundary of S_k, $k = 0, 1, 2, \ldots$. Thus, $\ell' = \ell = 0$, $m' = m - 1 = 4^k$, and the generalized condenser reduces to a classical condenser. The field of the condenser, G, is then the bounded multiply connected domain in the exterior of the closed sets S_k and in the interior of the circle $|z - (0.5 + 0.5\mathrm{i})| = 1$ (see Fig. 7).

The approximate value of the capacity for $k = 0, 1, \ldots, 5$ are shown in Table 4 and the level curves of the function u for $k = 1, 2$ are shown in Fig. 7. As in the previous example, the presented method is used with $n = 2^9$.

8. Numerical examples - generalized condensers

In this section, we shall consider several numerical examples of generalized condensers. For such a case, we have either $\ell \neq 0$ or $\ell = 0$ with $\{\delta_k\}_{k=1}^m$ containing at least three different numbers.

8.1. Six circles

In this example, we assume that $E = \{E_1, E_2\}$ where E_1 and E_2 are as in Section 7.1 with $a = 2$, i.e., $E_1 = \overline{G_1}$ with $G_1 = \{z : |z| < 1\}$, and $E_2 = \overline{G_2}$ with $G_2 = \{z : |z - 2| < r\}$ where $0 < r < 1$ (and hence $m' = m = 2$). We consider the generalized condenser $C = (B, E, \delta)$ where $\delta = \{0, \delta_2\}$ with a non-zero real number δ_2 for two cases of the domain B.

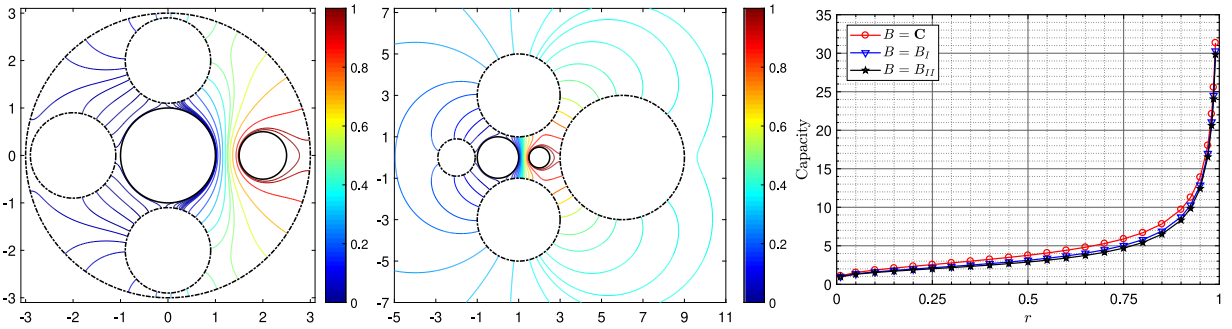

Fig. 8. The field of the condenser and the level curves of the function u for $B = B_I$ (left) and $B = B_{II}$ (center); and the approximate values of the capacity for $\delta_2 = 1$ (right).

Table 5
The approximate values of the capacity cap(C) for Section 8.1.

δ_2	$B = B_I$	$B = B_{II}$	$B = \mathbb{C}$
0.15	0.070116283201223	0.064979770350752	0.084657798864524
0.30	0.280465132804894	0.259919081403007	0.338631195458096
0.45	0.631046548811011	0.584817933156765	0.761920189780715
0.60	1.121860531219576	1.039676325612028	1.354524781832383
0.15	1.752907080030588	1.624494258768793	2.116444971613098
0.90	2.524186195244046	2.339271732627063	3.047680759122861

First, we assume that B is the bounded multiply connected domain

$$B = B_I = \{z : |z| < 3, \quad |z+2| > 0.9, \quad |z \mp 2\mathrm{i}| > 0.9\}.$$

Hence $\ell = 4$ and $\ell' = 3$. The field of the condenser, G, is then the bounded multiply connected domain of connectivity 6 exterior to the circles $\Gamma_1 = \{z : |z| = 1\}$, $\Gamma_2 = \{z : |z-2| = r\}$, $\Gamma_2' = \{z : |z-2| = r\}$, $L_{1,2} = \{z : |z \mp 2i| = 0.9\}$, $L_3 = \{z : |z+2| = 0.9\}$, and interior to the circle $L_4 = \{z : |z| = 3\}$ (see Fig. 8 (left) for $r = 0.5$).

Second, we assume that B is the unbounded multiply connected domain

$$B = B_{II} = \{z : |z-6| > 3, \quad |z+2| > 0.9, \quad |z-(1 \pm 3\mathrm{i})| > 2\}.$$

and hence $\ell' = \ell = 4$. Thus, G is the unbounded multiply connected domain of connectivity 6 exterior to the circles $\Gamma_1 = \{z : |z| = 1\}$, $\Gamma_2 = \{z : |z-2| = r\}$, $L_{1,2} = \{z : |z-(1 \pm 3\mathrm{i})| = 2\}$, $L_3 = \{z : |z+2| = 0.9\}$, and $L_4 = \{z : |z-6| = 3\}$ (see Fig. 8 (center) for $r = 0.5$).

As in Section 7.1, we use the presented method with $n = 2^{10}$. The approximate values of the capacity computed for $r = 0.5$ and for several values of δ_2 are presented in Table 5. The level curves of the function u for $r = 0.5$ and $\delta_2 = 1$ are shown in Fig. 8 (left, center). Fig. 8 (right) shows the approximate values of the capacity computed for $\delta_2 = 1$ and for several values of r between 0.01 and 0.99. We see from Table 5 and Fig. 8 (right) that the capacity of the condenser $C = (B, E, \delta)$ for $B = B_I$ and $B = B_{II}$ is less than the capacity for $B = \mathbb{C}$ (Section 7.1).

8.2. Five circles

In this example, we consider the generalized condenser $C = (B, E, \delta)$ with $B = \mathbb{C}$, $E = \{E_1, \ldots, E_5\}$, and $\delta = \{1, 2, 3, 4, 0\}$. The plates of the condenser are given by $E_k = \overline{G_k}$, $k = 1, \ldots, m$, where $G_{1,3} = \{z : |z \mp 2| < 1\}$, $G_{2,4} = \{z : |z \mp 2\mathrm{i}| < r\}$, and $G_5 = \{z : |z| > 4\}$. So, $\ell' = \ell = 0$, $m = 5$, and $m' = 4$. The field of the condenser, G, is then the bounded multiply connected domain in the exterior of the four circles $\Gamma_{1,3} = \{z : |z \mp 2| = 1\}$ and $\Gamma_{2,4} = \{z : |z \mp 2\mathrm{i}| = 1\}$; and in the interior of the circle $\Gamma_5 = \{z : |z| = 4\}$ (see Fig. 9).

The approximate values of the capacity obtained with several values of n are shown in Table 6. Fig. 9 shows the level curves of the function u obtained with $n = 2^{10}$.

8.3. Sierpinski carpet

The Sierpinski carpet is another generalization of the Cantor set to dimension two. The construction of the Sierpinski carpet begins with a square S_0. The square S_0 is subdivided into 9 congruent subsquares in a 3-by-3 grid, and the central subsquare is removed to obtain S_1. Then, we subdivide each of the 8 remaining solid squares into 9 congruent squares

Table 6
The approximate values of the capacity cap(C) for Section 8.2.

n	cap(C)
2^5	140.5271930046695
2^6	140.5271935663499
2^7	140.5271935663502
2^8	140.5271935663485
2^9	140.5271935663483
2^{10}	140.5271935663559

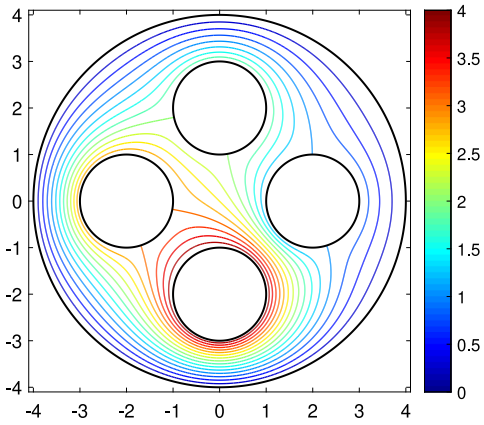

Fig. 9. The field of the condenser and the level curves of the function u for the condenser in Section 8.2.

and remove the center square from each to obtain S_2. The same procedure is then applied recursively to obtain $S_3, S_4, \ldots$, where

$$S_0 \supset S_1 \supset S_2 \supset S_3 \supset S_4 \supset \cdots,$$

(see Fig. 10 for S_2 (left) and S_3 (right)). Then the Sierpinski carpet is defined as

$$S = \bigcap_{k=0}^{\infty} S_k.$$

For $k = 0, 1, 2, \ldots$, the domain $\hat{S}_k = S_k \backslash \partial S_k$ is a multiply connected domain of connectivity $1 + \sum_{j=0}^{k} 8^j$. The domain $\hat{S}_k$ has $1 + \sum_{j=0}^{k} 8^j$ boundary components which all are squares. We will distinguish here two of these squares, namely, the external square which will be called Γ_2 and internal square which was removed from S_0 to obtain S_1 and it will be called Γ_1. The other $-1 + \sum_{j=0}^{k} 8^j$ squares are in the domain between Γ_1 and Γ_2. Let B be the multiply connected domain obtained by removing these $-1 + \sum_{j=0}^{k} 8^j$ squares and the domains interior to these squares from the extended complex place $\hat{\mathbb{C}}$. Let also $E_1 = \overline{G}_1$ where G_1 is the domain interior to Γ_1 and $E_2 = \overline{G}_2$ where G_2 is the domain exterior to Γ_2. In this example, we consider the generalized condensers $C_k = (B, E, \delta)$ with $E = \{E_1, E_2\}$ and $\delta = \{0, 1\}$. Thus, $\ell' = \ell = -1 + \sum_{j=0}^{k} 8^j$, $m = 2$, and $m' = 1$. The field of the condenser, G, is then the bounded multiply connected domain $\hat{S}$ (see Fig. 10).

The approximate values of the capacity for $k = 0, 1, 2, 3, 4$ are shown in Table 7 and the level curves of the function u for $k = 2, 3$ are shown in Fig. 10. The presented method is used with $n = 2^{10}$. For this example, we have $m' = 1$ and hence we need to solve only one integral equation to compute cap(C_k) for each k. The presented method can be used to compute the capacity even when the number of squares is very high. For example, to compute cap(C_k) for $k = 5$, the connectivity of the domain G is 4682 and hence, for $n = 2^{10}$, the size of the linear system obtained by discretization the integral equation is 4794368 by 4794368. Although the size of the system is very high, the presented method requires only 400 seconds to compute the capacity.

9. Condensers with slit plates

The method presented above can be used to compute the capacity of only condensers bordered by smooth or piecewise smooth boundaries. Since the Dirichlet integral is conformally invariant, the capacities for the cases for which the plates of the condenser are rectilinear slits can be computed with the help of conformal mappings as in the following examples.

Table 7
The approximate values of the capacity $\text{cap}(C_k)$ for Section 8.3.

k	$m+\ell$	$\text{cap}(C_k)$	CPU time (sec)
1	2	6.215546324111108	0.25
2	10	5.088779139415422	0.64
3	74	4.076130615454810	3.00
4	586	3.258035364401146	29.69
5	4682	2.600902059654094	399.97

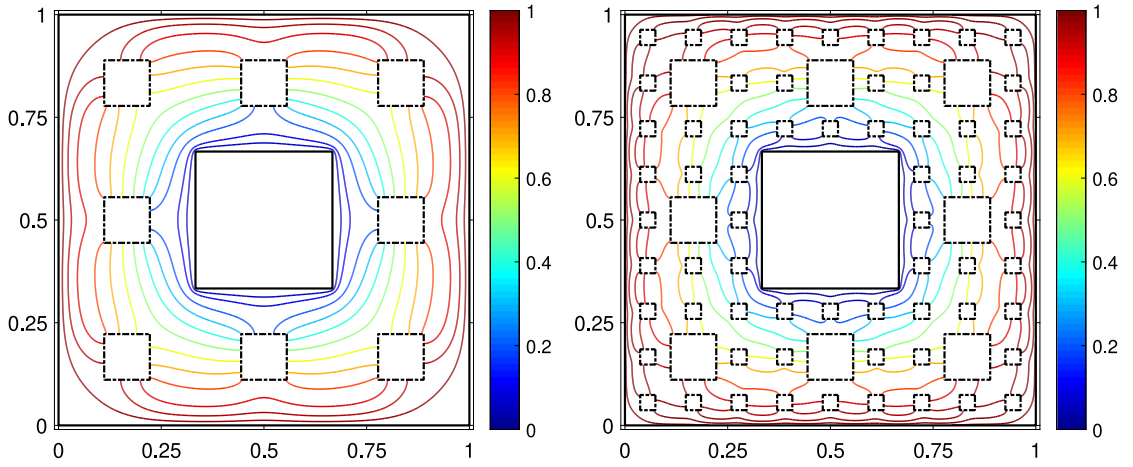

Fig. 10. The level curves of the function u for the condenser in Section 8.3 for $k = 2$ (left) and $k = 3$ (right).

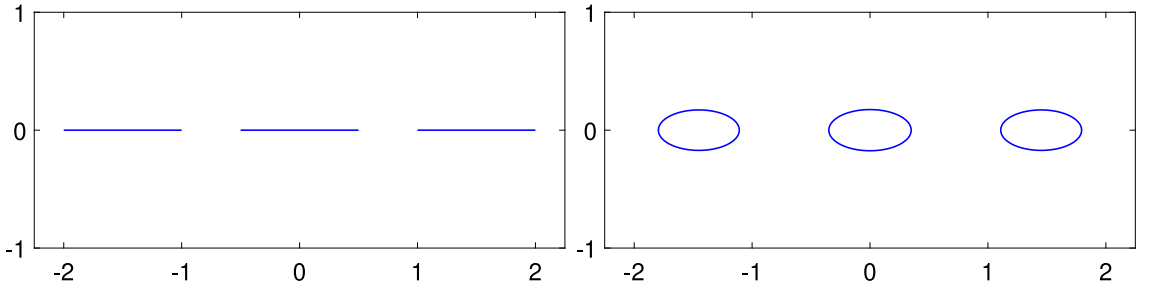

Fig. 11. The domains G (left) and $\hat{G}$ (right) for the condenser in Section 9.1.

9.1. Three slits: classical condenser

In this example, we consider the generalized condenser $C = (B, E, \delta)$ with $B = \mathbb{C}$, $E = \{E_1, E_2, E_3\}$ where $E_1 = [-c, -1]$, $E_2 = [a, b]$, and $E_3 = [1, c]$, $-1 < a < b < 1 < c$. For the levels of the potential of the plates, we consider two cases: $\delta = \{1, 1, 0\}$ and $\delta = \{0, 1, 0\}$. So, $\ell = 0$, $m = 3$, and the generalized condenser reduces to a classical condenser. This example has been considered in [9, Example 6] for several values of a and b.

Here, the field of the generalized condenser, G, is the unbounded triply connected domain in the exterior of the three slits E_1, E_2, and E_3 (see Fig. 11). Hence, the domain G for this generalized condenser is not bordered by Jordan curves. So, the method presented above is not directly applicable to such a domain G. Thus, to compute the capacity of this condenser, we first map this domain onto a domain $\hat{G}$ bordered by smooth Jordan curves so that our method can be used. An iterative numerical method for computing such a domain $\hat{G}$ has been presented recently in [37]. Using this iterative method, a conformally equivalent domain $\hat{G}$ bordered by ellipses can be obtained as in Fig. 11 (right). For details on the iterative method for computing the domain G, we refer the reader to [37].

Since the Dirichlet integral is conformally invariant, the capacity for the new domain $\hat{G}$ is the same as the capacity for the original domain G. For the new domain $\hat{G}$, we use the presented method with $n = 2^{11}$ for several values of the constants a, b, and c (for the same values used in [9]). The level curves of the function u for $a = -0.5$, $b = 0.5$, and $c = 2$ are shown in Fig. 12. The obtained approximate values of the capacity as well as the results presented in [9] are shown in Table 8.

Table 8
The approximate values of the capacity cap(C) for Section 9.1.

a	b	c	Case I		Case II	
			Our method	Betsakos et al. [9]	Our method	Betsakos et al. [9]
−0.9	0	2	1.708669509849820	1.7086693	3.453772340126319	3.4537720
−0.5	0.5	2	2.095326566730911	2.0953263	2.941023714396430	2.9410234
−0.9	0.9	2	3.067636432954407	3.0676361	5.187751867577839	5.1877511
0	0.9	2	3.033274793073555	3.0332745	3.453772340126327	3.4537719
−0.5	0.5	3	2.412575260903909	2.4125750	3.048687933334055	3.0486876
−0.7	0.2	3	2.131839309436634	2.1318391	3.017210220380872	3.0172100
0.5	0.8	3	2.807123923176794	2.8071236	2.312108724455613	2.3121085

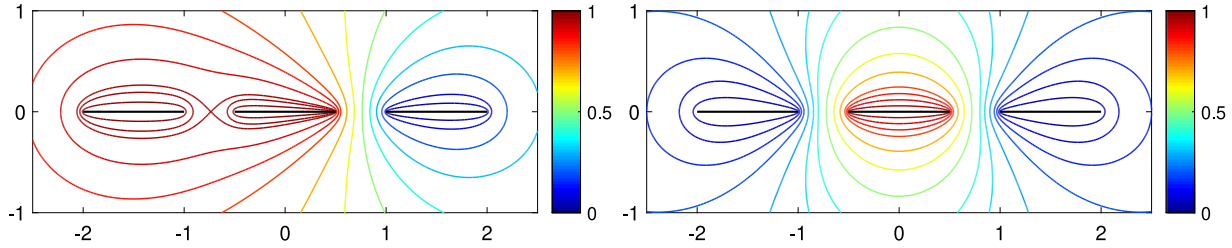

Fig. 12. The level curves of the function u for the condenser in Section 9.1 for Case I (left) and Case II (right).

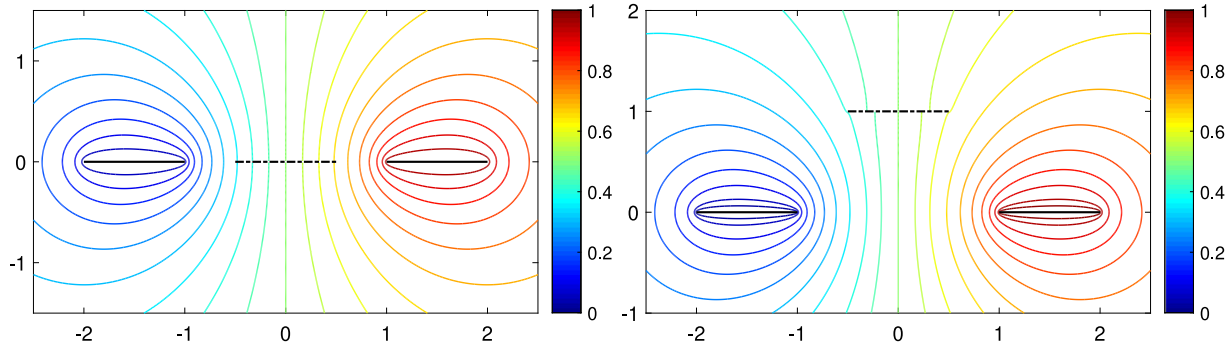

Fig. 13. The level curves of the function u for the condenser in Section 9.2 for $B = \mathbb{C}\backslash[a, b]$ (left) and $B = \mathbb{C}\backslash[a + \mathrm{i}, b + \mathrm{i}]$ (right).

9.2. Three slits: generalized condenser

In this example, we consider the generalized condenser $C = (B, E, \delta)$ with $B = \mathbb{C}\backslash[a, b]$, $E = \{E_1, E_2\}$ where $E_1 = [-c, -1]$, $E_2 = [1, c]$, and $\delta = \{0, 1\}$, $-1 < a < b < 1 < c$. So, here we have $\ell = 1$, $m = 2$. The domain G of condenser here is the same as in Section 9.1 and the Dirichlet boundary condition on the middle slit is replaced with the Neumann condition. Thus, as in Section 9.1, we compute first a conformally equivalent domain $\hat{G}$ bordered by smooth Jordan curves. Then, for the domain $\hat{G}$, we use the presented method with $n = 2^{11}$ for the same values of the constants a, b, and c used in Section 9.1. The obtained results are presented in Fig. 13 (left) and in Table 9.

We see from Table 9 that the middle segment $[a, b]$ on the real axis has no effect on the value of the capacity for this case. However, this will not be the case if we move the middle segment away from the real axis. To show that, we keep E and δ the same as above and we change the domain B to $B = \mathbb{C}\backslash[a + \mathrm{i}, b + \mathrm{i}]$, i.e., we move the middle segment vertically by unity. Then, the values of the capacity depends on a and b (see the fifth column in Table 9). The level curves of the potential function are presented in Fig. 13 (right).

9.3. Cantor set

In Section 7.3, we consider the Cantor dust which a generalization of the classical Cantor middle third set to dimension two. The boundaries of the closed sets S_k in Section 7.3 were piecewise smooth Jordan curves so the method presented in Section 6 is directly applicable to the problem considered in Section 7.3. In this example, we consider the classical

Table 9
The approximate values of the capacity cap(C) for Section 9.2.

a	b	c	$B = \mathbb{C}\backslash[a, b]$	$B = \mathbb{C}\backslash[a + \mathrm{i}, b + \mathrm{i}]$
−0.9	0	2	1.279261571170975	1.276631670192704
−0.5	0.5	2	1.279261571170975	1.278826082326995
−0.9	0.9	2	1.279261571170975	1.274579061435374
0	0.9	2	1.279261571170975	1.276631670192704
−0.5	0.5	3	1.563401922696102	1.563011913331686
−0.7	0.2	3	1.563401922696101	1.562502672069208
0.5	0.8	3	1.563401922696093	1.562906600728627

Table 10
The approximate values of the capacity cap(C_k) for Section 9.3.

k	$m = 2^k$	cap(C_k)	Time (sec)
1	2	1.563401922696121	0.22
2	4	1.521894262663735	0.70
3	8	1.498986233451143	2.17
4	16	1.487078427246902	6.84
5	32	1.480987379910617	23.20
6	64	1.477880583227881	91.26
7	128	1.476295519723391	371.64
8	256	1.475486275937497	1405.52
9	512	1.475072901005890	6158.92

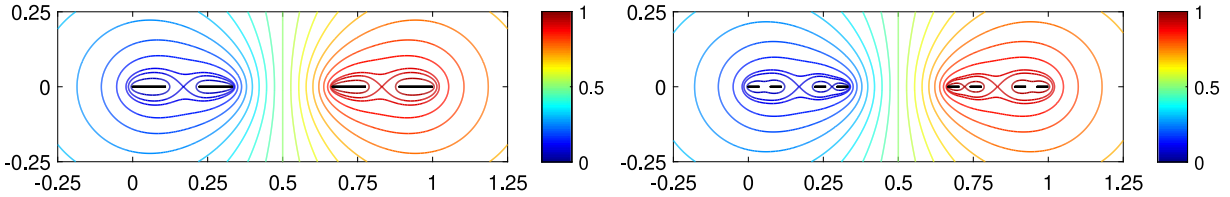

Fig. 14. The level curves of the function u for the condenser in Section 9.3 for $k = 2$ (left) and $k = 3$ (right).

Cantor middle third set and in this case the domain G is bordered by slits and hence the presented method is not directly applicable. However, the presented method can be used with the help of conformal mappings as explained in Section 9.1.

Let I_k, $k = 0, 1, 2, \ldots$, be as defined in Section 7.3. Then, the classical Cantor middle third set is defined as

$$I = \bigcap_{k=1}^{\infty} I_k.$$

For $k = 0, 1, 2, \ldots$, the closed set I_k consists of 2^k closed intervals $E_1, E_2, \ldots, E_{2^k}$ (see Fig. 14 for $k = 2$ (left) and $k = 3$ (right)). We consider the generalized condensers $C_k = (B, E, \delta)$ with $B = \mathbb{C}$ and $E = \{E_1, E_2, \ldots, E_{2^k}\}$. For the levels of the potential function $\delta = \{\delta_j\}_{j=1}^{4^k}$, we assume $\delta_j = 0$ for half of the plates (the plates on the left of the line $x = 0.5$) and $\delta_j = 1$ for the other half (the plates on the right of the line $x = 0.5$). Thus, $\ell = 0$, $m' = m = 2^k$, and the generalized condenser reduces to a classical condenser. The field of the condenser, G, is then the unbounded multiply connected domain in the exterior of the closed sets E_k (see Fig. 14).

The approximate values of the capacity for $k = 1, 2, \ldots, 9$ are shown in Table 10 and the level curves of the function u for $k = 2, 3$ are shown in Fig. 14. For each k, we need first to use the iterative method presented in [37] to compute a domain $\hat{G}$ bordered by smooth Jordan curves which is conformally equivalent to the domain G. Then, we use the presented method for the new domain $\hat{G}$ and the method requires solving $m = 2^k$ integral equations. The total CPU time for the two steps for each k is presented in Table 10. The presented numerical results were obtained with $n = 2^{10}$.

9.4. A rectangle with three slits: classical condenser

Two different analytical–numerical methods were applied in [8] for computing accurately the capacities of a wide family of symmetric condensers with complex geometry. In this example, to confirm the effectiveness and the accuracy of our proposed method, we consider the condenser A in [8, Fig. 4].

Let $C = (B, E, \delta)$ be the generalized condenser with $B = \mathbb{C}$, $E = \{E_1, E_2, E_3, E_4\}$, and $\delta = \{1, 1, 1, 1, 0\}$. The plates of the condenser are: $E_1 = [x_1, x_2]$, $E_2 = [x_3, x_4]$, $E_3 = [x_5, x_6]$, and $E_4 = \overline{G_4}$ where G_4 is the exterior of the square with the vertices $11 + Li$, Li, $-Li$, $11 - Li$. This example has been considered in [8, Fig. 4, Table 5] for several values of $x_1, \ldots, x_6, L$. We consider here the same values of $x_1, \ldots, x_6, L$ as shown in Table 11. For this example, $\ell' = \ell = 0$,

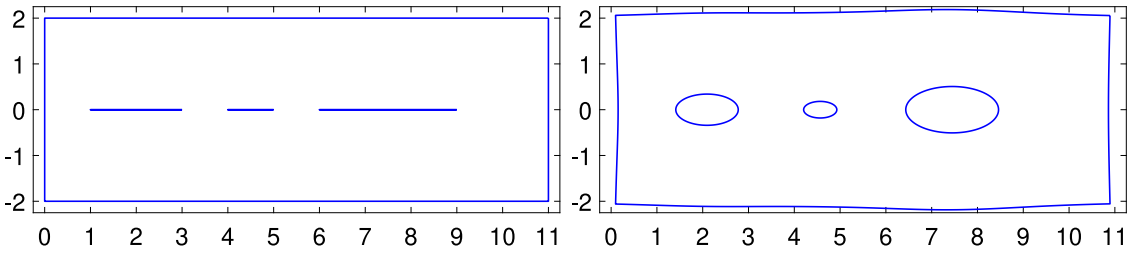

Fig. 15. The domains G (left) and $\hat{G}$ (right) for the condenser in Section 9.4 for the values of $x_1, \ldots, x_6, L$ given in Table 11 (Case I).

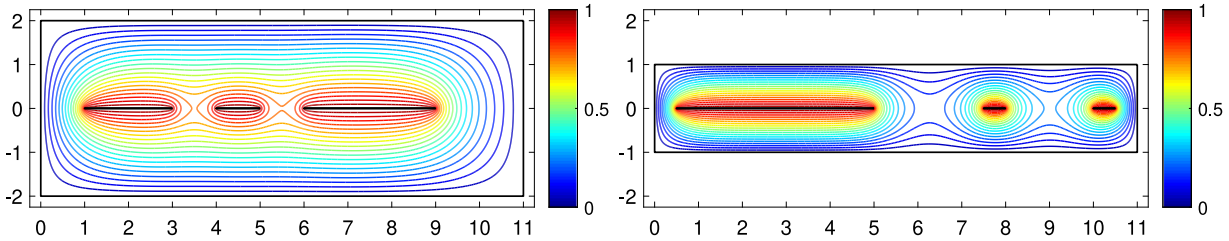

Fig. 16. The level curves of the function u for the condenser in Section 9.4 for the values of $x_1, \ldots, x_6, L$ given in Table 11: Case I (left) and Case III (right).

Table 11
The approximate values of the capacity cap(C) for Section 9.4.

Case	x_1	x_2	x_3	x_4	x_5	x_6	L	Our method	Bezrodnykh et al. [8]
I	1	3	4	5	6	9	2	9.720791206171137	9.72079120617096926
II	2	2.5	4.5	5	6	10.5	1	15.896403373409031	15.8964033734093744
III	0.5	5	7.5	8	10	10.5	1	16.570834992135438	16.5708349921371510
IV	1	1.5	2	8	10	10.5	3	9.077677435192859	9.0776774351927967
V	2	2.5	7.5	8	9	10.9	1	12.164276512644497	12.1642765126444534
VI	3	5	6	8	9	10	5	5.595178899111738	5.59517889911177450

$m = 4$, $m' = 3$, and the generalized condenser reduces to a classical condenser. The field of the condenser, G, is then the bounded quadruply connected domain in the exterior of the three slits E_1, E_2, E_3, and in the interior of the rectangle with the vertices $11 + Li$, Li, $-Li$, $11 - Li$ (see Fig. 15 (left)).

As the domain G for this condenser is not bordered by Jordan curves, the proposed method is not directly applicable. Thus, as in the previous three examples, to compute the capacity of this condenser, we will find a conformally equivalent quadruply connected domain $\hat{G}$ bordered by piecewise smooth Jordan curves so that our method can be used. First, as illustrated in Section 9.1, the iterative numerical method presented in [37] will be used to find a preimage domain in the exterior of three ellipses and a conformal mapping from this preimage domain onto the unbounded domain in the exterior of the three slits. Then, we use the inverse conformal mapping to map the rectangle onto a piecewise smooth Jordan curve enclosing the three ellipses. Thus, we obtain a conformally equivalent domain $\hat{G}$ in the interior of a piecewise smooth Jordan curve and in the exterior of three ellipses (see Fig. 15 (right)). For the new domain $\hat{G}$, we use the presented method with $n = 2^{11}$ for several values of $x_1, \ldots, x_6, L$ (we use the same values used in [8, Table 5]). The level curves of the function u for Cases I and III in Table 11 are shown in Fig. 16. The obtained approximate values of the capacity as well as the results presented in [8] are shown in Table 11 which illustrates that the results obtained using our method agreed with the results presented in [8].

10. Harmonic measure

Assume that the multiply connected domain G is as described in Section 2 with $\ell = 0$, i.e., G is a multiply connected domain of connectivity m bordered by $\Gamma = \cup_{k=1}^{m} \Gamma_k$ where Γ_m is the external boundary component if G is bounded. In this section, we shall use the method described above to compute the "harmonic measure" for the multiply connected domain G.

For a fixed j, $j = 1, 2, \ldots, m$, let u be the harmonic function in G that satisfy the boundary condition

$$u(\zeta) = \begin{cases} 1, & \zeta \in \Gamma_j, \\ 0, & \zeta \in \Gamma_k, \quad k \neq j, \quad k = 1, 2, \ldots, m, \end{cases} \tag{55}$$

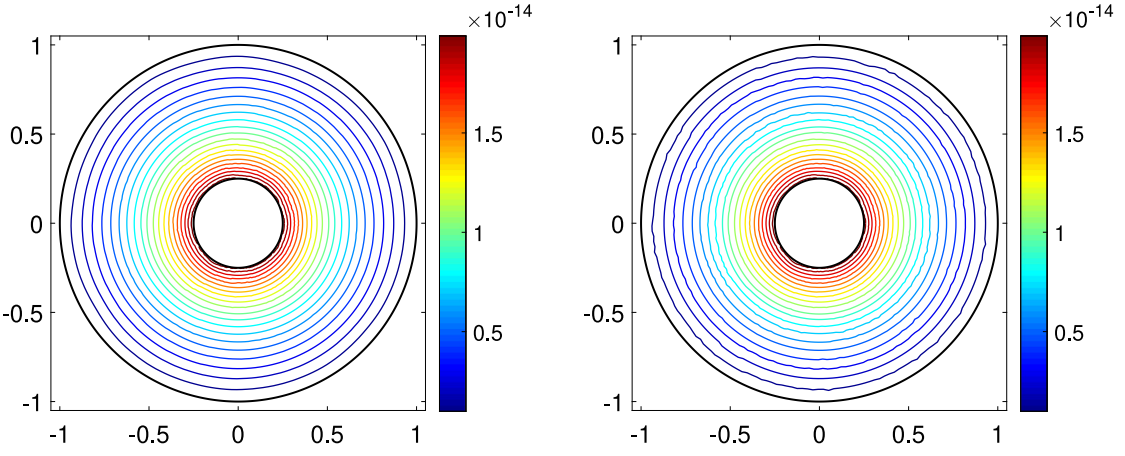

Fig. 17. The level curves of the absolute error in the computed values of the harmonic measures $\omega_{G,\Gamma_1}(z)$ (left) and $\omega_{G,\Gamma_2}(z)$ (right) for Section 10.1.

where u is assumed to be bounded at ∞ for unbounded G. Then the function u is called the harmonic measure of Γ_j with respect to G and will be denoted by ω_{G,Γ_j} [13,45–47]. From the Maximum Principle for harmonic functions [47, p. 77] it follows that $0 < \omega_{G,\Gamma_j}(z) < 1$ for $z \in G$. The harmonic measure $\omega_{G,\Gamma_j}(z)$ is invariant under conformal maps. If Φ is a conformal mapping from the domain G onto $\Phi(G)$, then [2,13]

$$\omega_{G,\Gamma_j}(z) = \omega_{\Phi(G),\Phi(\Gamma_j)}(\Phi(z))$$

for all $z \in G$, $j = 1, 2, \ldots, m$.

The boundary condition (55) is a special case of the boundary condition (4) (here, $\ell = 0$ so we will not have the normal derivative boundary condition). Thus, the algorithm presented in Section 5.4 can be used to compute the harmonic measure $\omega_{G,\Gamma_j}(z)$ for $z \in G$, $j = 1, 2, \ldots, m$. In fact, by the definition of the function δ in Section 9.1, the level curves presented in Fig. 12 (right) are the level curves of the harmonic measure $\omega_{G,\Gamma_2}(z)$ for the triply connected domain G in the exterior of the three slits Γ_1 (the left slit), Γ_2 (the middle slit), and Γ_3 (the right slit). The level curves presented in Fig. 12 (left) are the level curves of the sum of the harmonic measures $\omega_{G,\Gamma_1}(z) + \omega_{G,\Gamma_2}(z)$.

Below we consider three more examples.

10.1. Annulus

Let G by the annulus $G = \{z \in \mathbb{C} : q < |z| < 1\}$. Then the exact harmonic measures of the inner circle $\Gamma_1 = \{z \in \mathbb{C} : |z| = q\}$ and the outer circle $\Gamma_2 = \{z \in \mathbb{C} : |z| = 1\}$ with respect to G are given by

$$\omega_{G,\Gamma_1}(z) = \frac{\log|z|}{\log q}, \quad \omega_{G,\Gamma_2}(z) = 1 - \frac{\log|z|}{\log q}, \quad z \in G.$$

We use the method presented in Section 6 with $n = 2^{10}$ to compute approximate values of the harmonic measures $\omega_{G,\Gamma_1}(z)$ and $\omega_{G,\Gamma_2}(z)$ for $z \in G$. The absolute error in the computed values is shown in Fig. 17.

10.2. Two disks and two polygons

We consider the multiply connected domain G of connectivity 4 in the exterior of the curves $\Gamma_1, \Gamma_2, \Gamma_3$ and in the interior of the curve Γ_4. Here, Γ_1 is the circle $|z - 0.5| = 0.25$, Γ_2 is the circle $|z + 0.5| = 0.25$, Γ_3 is the polygon with the vertices $0.5 - 0.5\mathrm{i}$, $0.5 - 0.8\mathrm{i}$, $-0.5 - 0.8\mathrm{i}$, $-0.5 - 0.5\mathrm{i}$, and Γ_4 is the polygon with the vertices 1, i, -1, $-1 - \mathrm{i}$, $1 - \mathrm{i}$. We use the method presented in Section 6 with $n = 5 \times 2^8$ to compute approximate values of the harmonic measures $\omega_{G,\Gamma_1}(z)$, $\omega_{G,\Gamma_2}(z)$, $\omega_{G,\Gamma_3}(z)$ and $\omega_{G,\Gamma_4}(z)$ for $z \in G$. The level curves of the computed harmonic measures are shown in Fig. 18.

10.3. Cantor set

In this example, we compare our method with Trefethen's method [48] for solving the Laplace problem using series. For the definition of the Cantor middle third set, we use here the same definition employed in [48, § 5] which is equivalent to the definition given in Section 9.3. Let $I_0 = [-1.5, 1.5]$ and recursively define

$$I_k = \left(\frac{1}{3}I_{k-1} - 1\right) \cup \left(\frac{1}{3}I_{k-1} + 1\right), \quad k \geq 1.$$

Then, as in Section 9.3, the closed set I_k consists of 2^k closed intervals for each $k = 0, 1, 2, \ldots$.

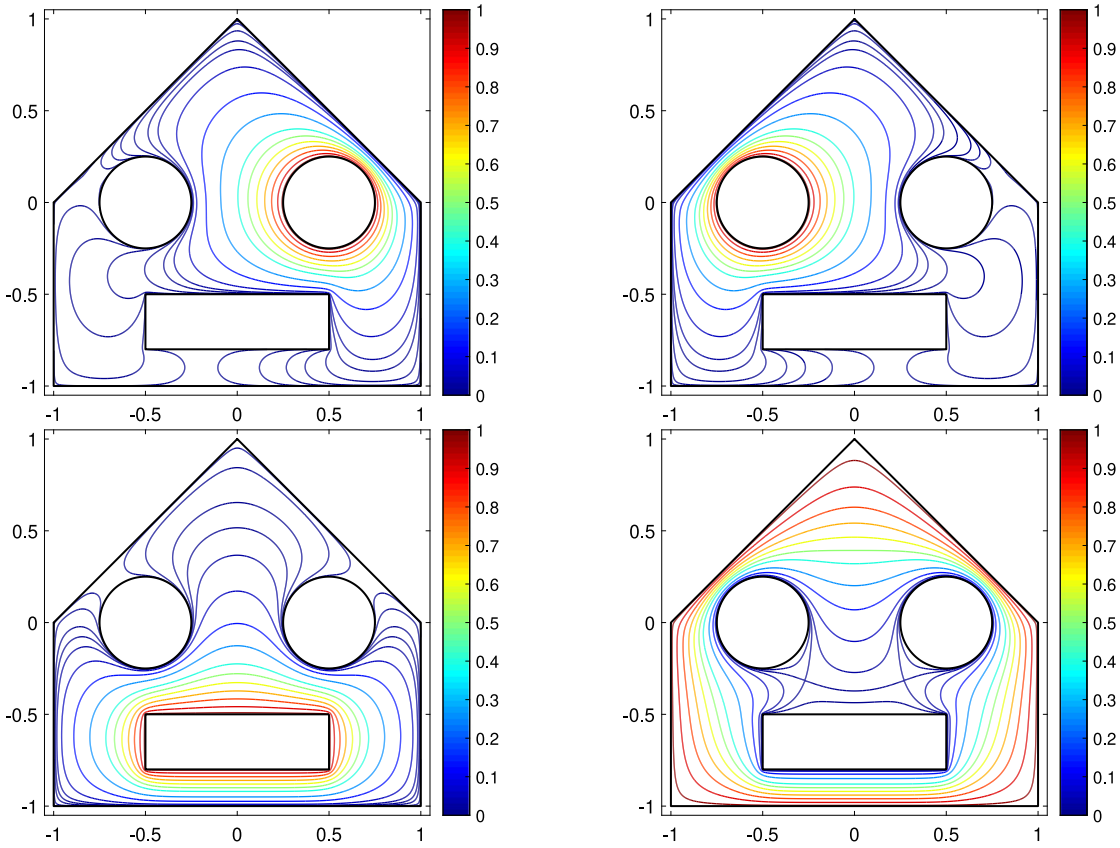

Fig. 18. The level curves of the computed harmonic measures $\omega_{G,\Gamma_1}(z)$ (top, left), $\omega_{G,\Gamma_2}(z)$ (top, right), $\omega_{G,\Gamma_3}(z)$ (bottom, left), and $\omega_{G,\Gamma_4}(z)$ (bottom, right) for Section 10.2.

Let G be the unbounded multiply connected domain of connectivity $m = 2^k$ in the exterior of I_k. As in [48], we assume that $\hat{I}$ is the union of the $m/2$ slits that are close to the origin from both sides (the slits between -1 and 1 in Fig. 19). Then, we consider the harmonic measure $\omega_{G,\hat{I}}(z)$, i.e., the harmonic function which equals 1 on the $m/2$ slits $\hat{I}$ and equals zero in the remaining slits. Since the harmonic measure is conformally invariant, the method presented in Section 6 combined with conformal mappings can be used to compute $\omega_{G,\hat{I}}(z)$ as explained in Sections 9.1 and 9.3. The level curves of the computed harmonic measure $\omega_{G,\hat{I}}(z)$ obtained with $n = 512$ (the number of nodes in the discretization of each boundary component) for $k = 2, 4, 6, 8$ are shown in Fig. 19.

The real number $\omega_{G,\hat{I}}(0)$ is known as the harmonic measure of $\hat{I}$ with respect to the basepoint $z = 0$ [49]. The real constant $\omega_{G,\hat{I}}(0)$ can be computed using the MATLAB function `cantor` in [48]. Table 12 presents the values of $\omega_{G,\hat{I}}(0)$ for several values of k obtained with the function `cantor`. These results are obtained by choosing the number of expansion terms and sample points in `cantor` to be 4. Note that, the numbers presented in the last two lines of Page 9 in [48] represent the harmonic measures of only half of the slits in $\hat{I}$ with respect to the basepoint $z = 0$, namely the slits on the positive real axis. Due to the symmetry of the domain, the harmonic measures of $\hat{I}$ with respect to the basepoint $z = 0$ are obtained by doubling the values in [48].

For comparison with the method presented in [48], we compute $\omega_{G,\hat{I}}(0)$ using our presented method with $n = 16$ and $n = 32$. The obtained numerical results are presented in Table 12. This table illustrated that there is a good agreement between the results obtained using MATLAB function `cantor` from [48] and our results even for values of n as small as $n = 16$. Further, the numerical results obtained with $n = 16$ and $n = 32$ are almost identical which indicates that using $n = 16$ is enough to compute $\omega_{G,\hat{I}}(0)$ to a good accuracy.

Acknowledgments

The authors would like to thank two anonymous referees for their valuable comments and suggestions which improved the presentation of this paper.

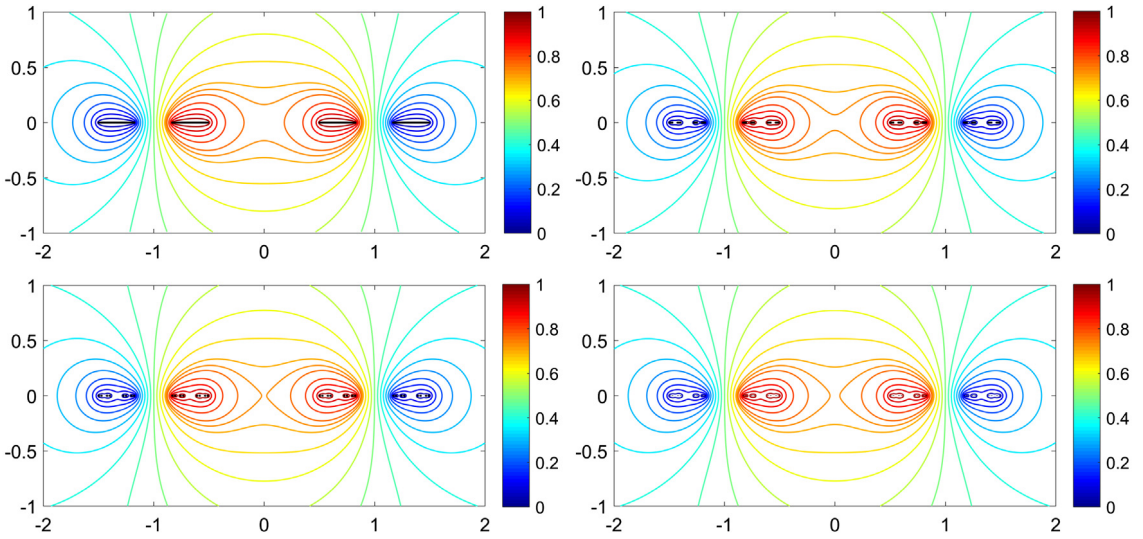

Fig. 19. The level curves of the computed harmonic measures $\omega_{G,i}(z)$ for $k = 2$ (top, left), $k = 4$ (top, right), $k = 6$ (bottom, left), and $k = 8$ (bottom, right) for Section 10.3.

Table 12
The approximate values of $\omega_{G,i}(0)$.

k	$m = 2^k$	Our method $(n = 16)$	Our method $(n = 32)$	Trefethen [48]
2	4	0.735551539985 19	0.735551539985189	0.735551540112459
3	8	0.729929583133879	0.729929583133878	0.729929583038891
4	16	0.727024871160416	0.727024871160416	0.727024871113871
5	32	0.725545991954976	0.725545991954976	0.72554599193114
6	64	0.724793400281699	0.724793400281699	0.724793400269526
7	128	0.724409827677884	0.724409827677885	0.724409827671667
8	256	0.724214086601555	0.724214086601554	0.724214086598381
9	512	0.724114119558644	0.724114119558644	0.724114119557021
10	1024	0.724063042631302	0.724063042631301	0.724063042630471
11	2048	0.724036939209317	0.724036939209316	0.724036939208896
12	4096	0.724023597064085	0.724023597064085	0.724023597063866

Appendix. The MATLAB function `capgc`

```
function [cap , uz] = capgc(et,etp,alphav,deltav,m,mp,ell,alpha,z)

ellp = ell ; ellp(abs(alpha)<inf & mp==m)=ell-1;
n=length(et)/(m+ell); tht=zeros(size(et)); tht(m*n+1:end)=pi/2;
if mp==m & ellp==ell
    A=exp(-i.*tht);
else
    A=exp(-i.*tht).*(et-alpha);
end
for k=1:mp
    for j=1:m+ell
        jv = 1+(j-1)*n:j*n;
        if (ellp==ell)
            gamk{k}(jv,1)=real(exp(-i.*tht(jv)).*clog(et(jv)-alphav(k)));
        else
            gamk{k}(jv,1)=real(exp(-i.*tht(jv)).*...
                clog((et(jv)-alphav(k))./(et(jv)-alpha)));
        end
    end
    [mu{k},h{k}]=fbie(et,etp,A,gamk{k},n,5,[],1e-14,100);
    for j=1:m+ell
        hjk(j,k)=mean(h{k}(1+(j-1)*n:j*n));
    end
```

```
end
mat=hjk; mat(1:m,mp+1)=1; mat(m+1:m+ell,mp+1)=0;
mat(1:m,mp+2:mp+ell+1)=0; mat(m+1:m+ell,mp+2:mp+ell+1)=-eye(ell);
rhs(1:m,1)=deltav; rhs(m+1:m+ell,1)=0;
if mp==m
    mat(m+ell+1,1:m)=1; mat(m+ell+1,m+1:m+ell+1)=0; rhs(m+ell+1,1)=0;
end
x=mat\rhs; a=x(1:mp,1); c=x(mp+1);
if mp==m-1
    a(m,1)=-sum(a);
end
cap  = (2*pi)*sum(deltav(:).*a(:));
if nargin==9
    fet = zeros(size(et)); uz=zeros(size(z));
    for k=1:mp
        fet = fet+a(k).*(gamk{k}+h{k}+i.*mu{k})./A;
        uz=uz-a(k)*log(abs(z-alphav(k)));
    end
    if abs(alpha)<inf
        fz=fcau(et,etp,fet,z);
        uz=uz+c+real((z-alpha).*fz);
    else
        fz=fcau(et,etp,fet,z,n,0);
        uz=uz+c+real(fz);
    end
end
end
```

References

[1] L. Ahlfors, Conformal invariants, McGraw-Hill, New York, 1973.
[2] G.D. Anderson, M.K. Vamanamurthy, M. Vuorinen, Conformal invariants, inequalities and quasiconformal maps, John Wiley, New York, 1997.
[3] T. DeLillo, A. Elcrat, E. Kropf, Calculation of resistances for multiply connected domains using Schwarz-Christoffel transformations, Comput. Methods Funct. Theory 11 (2011) 725–745.
[4] V. Dubinin, Condenser Capacities and Symmetrization in Geometric Function Theory, Springer, Basel, 2014.
[5] R. Kühnau, The conformal module of quadrilaterals and of rings, in: R. Kühnau (Ed.), Handbook of Complex Analysis: Geometric Function Theory, Vol. 2, Elsevier, Amsterdam, 2005, pp. 99–129.
[6] N. Papamichael, N. Stylianopoulos, Numerical Conformal Mapping: domain Decomposition and the Mapping of Quadrilaterals, World Scientific, New Jersey, 2010.
[7] A. Vasil'ev, Moduli of Families of Curves for Conformal and Quasiconformal Mappings, Springer-Verlag, Berlin, 2002.
[8] S. Bezrodnykh, A. Bogatyrev, S. Goreinov, O. Grigoriev, H. Hakula, M. Vuorinen, On capacity computation for symmetric polygonal condensers, J. Comput. Appl. Math. 361 (2019) 271–282.
[9] D. Betsakos, K. Samuelsson, M. Vuorinen, The computation of capacity of planar condensers, Publ. Inst. Math. (Beograd) (N.S.) 75 (89) (2004) 233–252.
[10] H. Hakula, A. Rasila, M. Vuorinen, On moduli of rings and quadrilaterals: algorithms and experiments, SIAM J. Sci. Comput. 33 (2011) 279–302.
[11] H. Hakula, A. Rasila, M. Vuorinen, Computation of exterior moduli of quadrilaterals, Electron. Trans. Numer. Anal. 40 (2013) 436–451.
[12] V. Dubinin, Capacities of condensers, generalizations of Grötzsch lemmas, and symmetrization, J. Math. Sci. 143 (2007) 3053–3068.
[13] J. Garnett, D. Marshall, Harmonic measure, Cambridge University Press, Cambridge, 2008.
[14] M. Vuorinen, Conformal Geometry and Quasiregular Mappings, Springer-Verlag, Berlin, 1988.
[15] J. Liesen, O. Séte, M. Nasser, Fast and accurate computation of the logarithmic capacity of compact sets, Comput. Methods Funct. Theory 17 (2017) 689–713.
[16] T. Ransford, Computation of logarithmic capacity, Comput. Methods Funct. Theory 10 (2) (2010) 555–578.
[17] T. Ransford, J. Rostand, Computation of capacity, Math. Comp. 76 (259) (2007) 1499–1520.
[18] V. Dubinin, N. Eyrikh, Applications of generalized condensers to analytic function theory, J. Math. Sci. 133 (2006) 1634–1647.
[19] V. Dubinin, D. Karp, Generalized condensers and distortion theorems for conformal mappings of planar domains, Contemp. Math. 424 (2007) 33–52.
[20] V. Dubinin, D. Karp, Capacities of certain plane condensers and sets under simple geometric transformations, Complex Var. Elliptic Equ. 53 (6) (2008) 607–622.
[21] M. Nasser, Fast solution of boundary integral equations with the generalized neumann kernel, Electron. Trans. Numer. Anal. 44 (2015) 189–229.
[22] R. Wegmann, M. Nasser, The Riemann-Hilbert problem and the generalized Neumann kernel on multiply connected regions, J. Comput. Appl. Math. 214 (2008) 36–57.
[23] S. Mikhlin, Integral Equations and Their Applications to Certain Problems in Mechanics, Mathematical Physics and Technolog, second ed., Pergamon Press, Oxford, 1964.
[24] P. Ivanshin, E.A. Shirokova, The solution of a mixed boundary value problem for the Laplace equation in a multiply connected domain, Probl. Anal. Issues Anal. 8 (26) (2019) 51–66.
[25] S. Al-Hatemi, A. Murid, M. Nasser, A boundary integral equation with the generalized Neumann kernel for a mixed boundary value problem in unbounded multiply connected regions, Bound. Value Probl. 2013 (2013) Article No. 54.
[26] M. Nasser, A. Murid, S. Al-Hatemi, A boundary integral equation with the generalized Neumann kernel for a certain class of mixed boundary value problem, J. Appl. Math. 2012 (2012) 254123.
[27] F. Gakhov, Boundary Value Problems, Pergamon Press, Oxford, 1966.
[28] N. Muskhelishvili, Singular Integral Equations, Noordhoff, Groningen, 1953.
[29] R. Haas, H. Brauchli, Fast solver for plane potential problems with mixed boundary conditions, Comput. Methods Appl. Mech. Engrg. 89 (1991) 543–556.

[30] S. Bezrodnykh, Lauricella hypergeometric function $F_D^{(N)}$, the Riemann-Hilbert problem and some applications, Russian Math. Surveys 73 (6) (2018) 941–1031.
[31] S. Bezrodnykh, V. Vlasov, The Riemann-Hilbert problem in a complicated domain for the model of magnetic reconnection in plasma, Comput. Math. Math. Phys. 42 (3) (2002) 263–298.
[32] M. Nasser, The Riemann-Hilbert problem and the generalized Neumann kernel on unbounded multiply connected regions, Univ. Res. (IBB University Journal) 20 (2009) 47–60.
[33] M. Nasser, A boundary integral equation for conformal mapping of bounded multiply connected regions, Comput. Methods Funct. Theory 9 (2009) 127–143.
[34] M. Nasser, Numerical conformal mapping of multiply connected regions onto the second, third and fourth categories of Koebe canonical slit domains, J. Math. Anal. Appl. 382 (2011) 47–56.
[35] M. Nasser, J. Liesen, O. Séte, Numerical computation of the conformal map onto lemniscatic domains, Comput. Methods Funct. Theory 16 (2016) 609–635.
[36] M. Nasser, Numerical conformal mapping via a boundary integral equation with the generalized Neumann kernel, SIAM J. Sci. Comput. 31 (2009) 1695–1715.
[37] M. Nasser, C. Green, A fast numerical method for ideal fluid flow in domains with multiple stirrers, Nonlinearity 31 (2018) 815–837.
[38] E. Nyström, Über die praktische Auflösung von Integralgleichungen mit Anwendungen auf Randwertaufgaben, Acta Math. 54 (1930) 185–204.
[39] K. Atkinson, The Numerical Solution of Integral Equations of the Second Kind, Cambridge University Press, Cambridge, 1997.
[40] L. Trefethen, J. Weideman, The exponentially convergent trapezoidal rule, SIAM Rev. 56 (2014) 385–458.
[41] L. Greengard, Z. Gimbutas, FMMLIB2D: A MATLAB toolbox for fast multipole method in two dimensions, Version 1.2, 2012. http://www.cims.nyu.edu/cmcl/fmm2dlib/fmm2dlib.html. (Accessed 1 January 2018).
[42] M. Nasser, A. Murid, M. Ismail, E. Alejaily, Boundary integral equations with the generalized Neumann kernel for Laplace's equation in multiply connected regions, Appl. Math. Comput. 217 (2011) 4710–4727.
[43] R. Kress, A Nyström method for boundary integral equations in domains with corners, Numer. Math. 58 (2) (1990) 145–161.
[44] G. Pólya, G. Szegö, Isoperimetric Inequalities in Mathematical Physics, Princeton University Press, Princeton, 1951.
[45] D. Crowdy, J. Marshall, Green's functions for Laplace equation in multiply connected domains, IMA J. Appl. Math. 72 (2007) 278–301.
[46] S. Krantz, Geometric Function Theory: Explorations in Complex Analysis, Birkhäuser, Boston, 2006.
[47] M. Tsuji, Potential Theory in Modern Function Theory, Chelsea Publ. Co., New York, 1975.
[48] L. Trefethen, Series solution of Laplace problems, ANZIAM J. 60 (2018) 1–26.
[49] M. Snipes, L. Ward, Harmonic measure distributions of planar domains: a survey, J. Anal. 24 (2016) 293–330.